

Vulnerability assessment of an innovative precast concrete sandwich panel subjected to the ISO 834 fire

K.J. Kontoleon^{a*}, K. Georgiadis-Filikas^a, K.G. Tsikaloudaki^a, T.G. Theodosiou^a,
C.S. Giarma^a, C.G. Papanicolaou^b, T.C. Triantafillou^b, E.K. Asimakopoulou^c

^a Laboratory of Building Construction & Building Physics, Department of Civil Engineering,
Faculty of Engineering, Aristotle University of Thessaloniki (AUTH),
University Campus, Gr-54124 Thessaloniki, Greece

^b Laboratory of Structural Materials, Department of Civil Engineering,
School of Engineering, University of Patras (UoP),
University Campus, Gr-26504 Patra, Greece

^c School of Engineering, University of Central Lancashire (UCLan),
University Campus, Fylde Rd, Preston PR1 2HE, United Kingdom

* e-mail (Corresponding Author): kontoleon@civil.auth.gr

Abstract

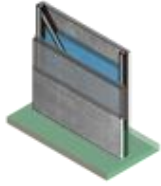
Development and use of preconstruction have been exhibited for several decades. Numerous modules, ranging from the simplest to the most advanced concepts, have been suggested to ameliorate the layout of building structures, with respect to a broad spectrum of needs. This study aims to unfold the fire defensiveness of an innovative precast concrete sandwich wall-system [subjected to the ISO 834 fire](#), such as this is provided for in EN1991-1-2. In light of a rapidly evolving environment that should shield structures against fire, this investigation emphasises on the vulnerability of precast panels with a varying thickness of insulation by means of a numerical methodology and a versatile [heat transfer-model](#). A finite-element analysis is carried out with COMSOL Multiphysics[®] simulation software. In a following step, as fire risk should be vigorously tackled, the research is extended to validate numerical predictions of the model by means of an experimental setup for wall specimens arranged in the laboratory. Therefore, an additional goal of this [research](#) is to assess temperature discrepancies for both addressed cases. Despite various approximations of the model, an excellent agreement between numerical and experimental results is shown, confirming the rationality of computational simulations in terms of temperatures' precision. It has been revealed that for all examined cases, the insulation ability (I) has been maintained for more than [3 hours](#) regardless of the positioning of the insulation. [Further evidence though suggested that is not the case for the loadbearing capacity \(R\)](#), as the installation of a fire exposed insulation layer resulted in lower stability systems. Also, the effect of the insulation thickness is not that dominant as on average and maximum temperature deviations among marginal assemblies ($d_{EPS} = 2$ cm and $d_{EPS} = 10$ cm) did not exceed 5 °C and 10 °C at $t_{fire} \approx 100$ min.

Keywords: Layered structures, High-temperature properties, [Finite Element Analysis \(FEA\)](#), [heat transfer](#), Fire Resistance

Graphical Abstract

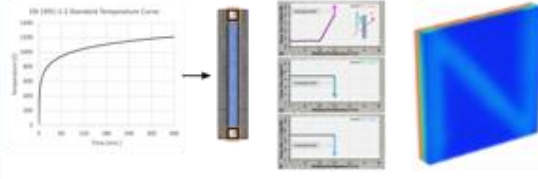
Scope

Thermal analysis of precast concrete sandwichwall system exposed to fire attack



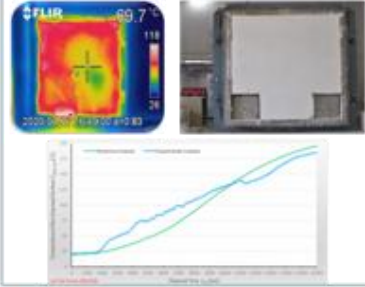
Methodology

- Adoption of temperature-dependent material properties
- Modelling technique for numerical treatment of EPS decomposition and render fall
- FEA-based simulations with respect to the thickness and position of EPS insulation



Validation

Model validation by means of a medium scale test



Nomenclature

d	thickness [m]
C_p	specific heat capacity [J/(kg·K)]
h	heat transfer coefficient [W/(m ² K)]
Q_{gen}	volumetric heat generation [W/m ³]
q	heat flux [W/m ²]
T	temperature [°C]
ΔT	temperature difference [°C]
t	time [s]
u	moisture content [%]

Subscripts	
amb	ambient air
$C25/30-vol$	volumetric average of concrete wythe exposed to fire
$conv$	convection
EPS	expanded polystyrene, as the one-side thermal insulation layer
$EPS-core$	expanded polystyrene, as the core thermal insulation layer
env	environment
exp	exposed to fire surface
$fire$	fire ambience
min / max	minimum / maximum
$mean-surf$	mean value of an unexposed to fire surface
$peak-surf$	peak value of an unexposed to fire surface
rad	radiation
$S235-vol$	volumetric average of steel tubing system between both wythes
$surf$	surface
$total$	overall effect due to combined convection and radiation
$unexp$	unexposed to fire surface

Greek Letters	
ϵ	emissivity [-]
λ	thermal conductivity [W/(m·K)]
ρ	bulk density [kg/m ³]
σ	Stefan–Boltzmann constant [5.6697×10^{-8} W/(m ² ·K ⁴)]
φ	view factor of fire enclosure configuration [-]

Acronyms	
R	insulation (temperature rise) criterion [min]
E	integrity criterion [min]
I	insulation criterion [min]
C25/30	lightly reinforced concrete with a characteristic compressive cylinder/cube strength of 25/30 N/mm ²
S235	steel square hollow structural sections (HSS) of structural carbon steel with a yield strength of 235 N/mm ²
EPS	expanded polystyrene
CbM	cement-based mortar

Contents

Abstract	1
Nomenclature	3
1. Introduction	5
1.1. Intuition of fire risk evinced by recent advances in preconstruction.....	5
1.2. Fundamental thresholds in precast design.....	5
1.3. Critical challenges alongside fire hazards.....	6
1.4. Focus and innovation of the current work.....	7
2. Methodology	8
2.1. Justification of buildings' fire safety in terms of fire resistance criteria	8
2.2. Fundamental mechanisms of heat transfer through a precast concrete sandwich panel.....	9
2.2.1. <i>Heat transfer boundary condition of an exposed to fire precast concrete sandwich panel</i>	11
2.2.2. Heat transfer boundary condition of a non-exposed to fire precast concrete sandwich panel	11
2.2.3. Nominal temperature-time curves	12
2.3. Analysed precast concrete sandwich panel system	12
2.3.1. Outline and variations of developed sandwich panel system	12
2.3.2. Thermophysical properties of involved materials under conventional conditions	14
2.3.3. Modelling procedure as regards temperature-dependent and time-dependent properties of materials	15
2.3.4. Datasets of studied configurations of the sandwich panel system	19
2.4. Numerical technique of the transient thermal analysis and experimental validation of the model	20
2.4.1. Formulation of Finite Element Analysis by adopting the Finite Element Method	20
2.4.2. Validation of the thermal model by means of a laboratory-based experiment	21
3. Results and discussion.....	24
3.1. Temperature increase on the non-fired side of the analysed sandwich panel system	24
3.2. Volumetric average temperature evolution of the steel tubing coupling system between both wythes ...	27
3.3. Volumetric average temperature evolution of the exposed to fire concrete wythe	27
3.4. Fire resistance predictions of analysed sandwich panel system.....	30
4. Conclusions	32

1. Introduction

1.1. Intuition of fire risk evinced by recent advances in preconstruction

During the past few decades, there is an increased tendency to develop and promote prefabricated wall panel systems used in a variety of systematised building applications [1, 2]. Manufacturing of building elements away from the construction site and assembly on site continues to evolve, and constructors in real-worlds engineering problems are getting more and more connected to those technologies than ever before. To accommodate their increased use, facilitate their installation and incorporation in the relevant structures, numerous approaches, guidelines, codes, and standards of various complexity levels, ranging from basic to highly sophisticated ones, have been developed and launched [2-4]. Up to this day, the fundamental principles of preconstruction strive to balance a wide variety of basic needs, including aesthetics, functionality, structural integrity, energy consciousness and sustainability in terms of environmental protection. These aspects, as well as the length of time to complete a structure and the overall cost, should be carefully considered to evade all fundamental constraints of preconstruction from conception through planning, design and construction phases. Within this framework, modular construction with precast products aims to bridge the gap between traditional and modern practice in the frame of an all-inclusive design approach that supports the layout of building structures [4-10]. As seen in the literature, successful application of industrialised building systems is predominantly driven by the expansion of innovative technologies that offer a wide range of advantages including construction speed, cost effectiveness, safety and reduced environmental impact [1, 4, 11].

Furthermore, if we look at the bigger picture, preconstruction should also shed light on safety issues of building entities. Building structures must confront risks during the operational phase, in an effective way that fulfils the highest safety criteria [12-14]. In this rapidly shifting built environment, during the planning process a major reliability and system safety component of precast systems is the impact of fire hazards. To ensure maximum safety for modular constructions with prefabricated elements, an accurate fire risk level estimation should be an integral part of a conscious design [15-22]. This challenge is particularly acute in the building sector context, in which a vast majority of fire events involve old constructions and, most frequently, reflect the deficiency of a prudent design to confront risks when the threat rises beyond a certain level [23-25].

In order to tackle with this problem, building designers and engineers focus on fire safety of building structures by means of an insightful design aiming to prevent the next tragedy. In this context, fire safety of buildings can be attained by leveraging both passive and active measures in order to achieve the pre-set safety goals of the design. Such kind of active fire protection measures, aiming to succeed a certain degree of safety for the built-up area, are mostly delineated by prescriptive-based approaches [26-29]. Traditional prescriptive approaches refer to the majority of cases as they appear to be easier to assimilate. In this circle, during the past few years fire norms and requirements have been changing slowly; new aspects have been rarely embedded but, still, the main notion remains the same. However, rationality in preconstruction beyond such tentative steps cannot be rapidly consolidated without taking into consideration the foreseen changes. On the one hand, performance-based strategies to assess fire risk are lately introduced [30-33]. Their utilisation is shown to be beneficial as their reliability in terms of accuracy is sharp. At the same time, exhaustive simulations unveil a feasible way to capture and highlight thermal map trends under the assumption of various fire scenarios. On the other hand, the ongoing shift of innovation in preconstruction underlines some very critical challenges [2, 3, 34-38]. As seen, an accelerating growing trend to introduce building systems, that may involve several thin layers and materials with a contradicting structural responsiveness and thermal behaviour under elevated temperature, is progressively shown. In addition, innovation by composite modules containing combustible layers appears to also increase fire spread and evolution. Accordingly, the current tendency toward innovation of building preconstruction should be cautiously examined to strike a fair balance for both active and passive measures. The above developments apparently reflect a possible way to compromise the often-conflicting fundamental requirements in preconstruction planning. Nevertheless, for precast composite modules their design should comply with current national directives.

1.2. Fundamental thresholds in precast design

The general outline of fire risk in conjunction with the design and construction of precast structural panels has been thoroughly discussed in several studies. Special attention is primarily given on the structural behaviour of composite precast systems. As stated in [34], the development and utilisation of advanced composite precast frame systems allows a rapid and almost effortless erection and structural efficiency of building assemblies. In

this holistic work, fundamentals with respect to the post-yield response of concrete and metal units were also exhibited to indicate how these two diverse materials are connected together to eliminate individual material drawbacks in terms of structural efficiency. Another critical aspect influencing the industrialized design, production and construction of precast concrete panels refers to the connection practice between adjacent concrete wythes. In [35], particular emphasis was placed on the strength and stiffness of precast insulated concrete sandwich panels, while comparing conventional connectors with advanced shear connectors made of steel, glass fibers and a reinforced polymer material. To determine the degree of the partial composite action in terms of structural vulnerability, several full-scale precast specimens were tested in the laboratory. Related work in this research field focusing on insulated precast concrete sandwich panels with thin steel plate connectors is given in [46]. In this work, a large experimental study was realised to evaluate how building cladding connectors of various dimensions (varying thickness and depth) can give rise to dissimilar load capacities, stiffnesses and failure modes. In addition, the insulation layer was shown to play a central role in preventing rotation in response to a shear load. Apart from this, a finite element analysis was performed to interpret the non-linear behaviour of the precast concrete element. It should be noted that the relevant scientific literature in [34-36] and the references quoted therein is quite extended; nevertheless, a detailed state-of-the-art on the matter evades the scope of this study.

Furthermore, when it comes to develop a lighter and thinner precast concrete module, a broad spectrum of structural, thermal and practical challenges should be cautiously prioritised. In [47], a novel precast sandwich panel system assembled by two thin fibre-reinforced concrete layers of high strength and a highly efficient thermal insulation layer in the middle, was deemed to succeed a tolerable equilibrium with regard to structural and thermal requirements; in that respect, all layers of the precast concrete sandwich panel system were mechanically connected and fixed together with fibre reinforced polymer grid connectors, in an effort to ensure composite action of the cladding element. Alternative materials referring to shear connections of precast designs, that facilitate shear load transfer across layers while also reducing localised heat flows, are comprehensively presented in [2, 3]. In terms of structural capacity and integrity, the applicability of sandwich panels for a broader range of building typologies was proved to fundamentally rely on the mechanical performance of shear connectors. Furthermore, special emphasis was also paid to the foundation of a thermally efficient precast cladding solution, as thin and lightweight wall build-ups are experiencing a resurgence in popularity. Therefore, while conventional steel connector types enhance the structural behaviour of panel systems, they can simultaneously reduce their performance in terms of thermal defensiveness. One of the main causes that contributes to thermal degradation of sandwich panel designs is the unsought heat flux in the region of shear connections, as they serve as thermal bridges across panels.

Although, several innovations have been successfully conceived to improve the weak points of precast design, such as novel vacuum insulated panels (VIPs) between concrete wythes [38] and modern shear connectors [2, 3, 35, 37], yet there are a few issues that should be further clarified. First of all, an urgent point pertains to the stability of wythes (dimensions and mass of concrete layers) and the strength of different connector types (dimensions and materials of conventional/sophisticated shear connectors), under lateral dynamic excitations such as earthquake and wind loading (individual and/or combined action). From this point of view, a loss of structural integrity below a certain level indicates a critical risk, as this localised or ample failure may cause single-sided or bilateral overturning of the concrete wythe(s) with probable fatal consequences. In the meanwhile, three-dimensional heat transfer through a precast cladding system should be warily contemplated as it seems to dominantly affect the spatial and temporal evolution of temperatures. The bottom line here is that the literature in this field highlights a need for further validation and interpretation of precast innovations. Hence, several pioneering precast solutions are still questionable, despite their higher cost compared to representative arrangements followed mostly.

1.3. Critical challenges alongside fire hazards

In addition, in the matter of dealing with elevated temperatures and more specifically a vigorous fire attack, a key aspect is to assess the thermal vulnerability of precast concrete wall structures. Despite the unique nature of fire, and the fact that it has been repeatedly accentuated as a grave risk, research on the fire involvement through precast concrete sandwich wall panels has not yet been exhaustively carried out. Findings from on-the-ground efforts reveal that there is enough space to stretch further the frontiers of awareness and bridge the research gap. At the same time, there are rising expectations as to what innovations in precast design can achieve and how this can be satisfied by contemporary fire regulations.

So far, the majority of fire investigations evaluating the transient temperature gradient within precast panels, focuses on the fire resistance and the thermo-structural performance of loadbearing sandwich assemblies subjected to one-sided fire [39-41]. The prediction of the temperature gradient within their volume and at different times of fire exposure is mostly succeeded by means of finite element analysis approximations, while the solution of the governing differential equations of the envisioned structural model is attained iteratively by using the nonlinear shooting method. Apart from numerical solutions of thermo-structural models and parametric studies verified through comparisons with experimental fire tests and other reliable models in the literature, several surveys devote oneself to uncover the mechanical behaviour of precast panels by applying large-scale fire testing with loading [42, 43]. It is worth mentioning here that an eloquent evaluation ranking of the fire performance is mainly based on an entrenched point of notion. Therefore, experimental measurements are undertaken by following the standard fire resistance testing procedure from EN1363-1 [44], referring to the well-known REI criteria (certification tests to decrypt resistance, integrity and insulation). Then again, for the bulk of cases the enforced temperature abides by the conditions of the Standard cellulosic time-temperature curve for building elements in ISO834-1 [45].

Although numerous studies are dedicated on the thermo-structural behaviour of loadbearing precast panel systems, there is still a need to justify and, moreover, adjust the performability of non-loadbearing assemblies. In light of the foregoing and with an eye to promote further building applications of precast design, several inquiries verify the rationality of thermal modelling techniques; thereby, our first and foremost concern is to avoid pitfalls evinced by interventions of their radical design. An associated work on this research topic that evocatively elucidates the thermal performance of 3D-printed concrete (3DPC) composite wall panels under elevated temperatures is given in [46]. Toward this goal, a numerical analysis has addressed the temperatures non-uniformity of 3DPC wall specimens, showing the performance of elements of a varying thickness, density and configuration (wall panels subjected to Standard fire conditions: solid, cavity, insulated-composite), by means of a validated heat transfer finite element model. Another related study [47], focuses on fireproofing and temperature distributions through lightweight sandwich panels due to a fire hazard. Within this experimental framework, a broad variety of aspects that may identify the field of application of such solutions has been thoroughly discussed. Special emphasis was placed on the fire resistance test procedure (as recommended in EN13501-2, EN1363-1 and EN1364-1 standards), for sandwich wall assemblies with a varying insulation encasement within the core and with a different fireproofing layer. In a similar fashion, the fire resistance performance of structural and non-structural concrete-PVC panels with polyvinyl chloride (PVC) stay-in-place (SIP) formwork has been examined in [48]. PVC SIP formwork panels were tested and compared to one another (on the basis of the ISO834-1 standard), in terms of structural stability and fire resistance time.

1.4. Focus and innovation of the current work

As it is clear, existing literature reveals that there is a missing piece within the context of fire dynamics of innovative precast panels and cladding assemblies throughout their lifespan. Breaking the vicious circle between precast design and fire safety explains why the necessity towards reining in the risks arising from innovation in preconstruction and from contagious disturbance of the initial temperature balance is still so prominent. Those critical challenges, along with few other rising concerns [49], exhibit the dire need to expand further the channel of awareness and bridge the dearth of knowledge in this field.

To this end, the present work focuses on a vulnerability assessment of innovative precast concrete sandwich panel typologies under a rigorous fire action, such as this is advocated in the EN1991-1-2 standard [50]. Analysed typologies refer to precast designs with an insulation layer encased between both adjacent concrete wythes and an additional one, with a varying thickness, placed on one-side of the proposed system. The exposed insulation layer serves as a thermal barrier across the entire surface of the panel; in this manner, occurring heat gains at the junctions between panel elements (linear thermal bridging) are substantially diminished if they have not already been absolutely eliminated. Against this background, a one-sided fire referring to the Standard and External fire temperature curve is applied on both sides of the precast design.

Allied to this notion, a numerical methodology has been realised by adopting a finite-element analysis of the transient thermal problem. In this context, numerical simulations by means of the developed thermal model are carried out with COMSOL Multiphysics® simulation software [51]. [The software has been previously validated for fire resistance and fire propagation in structural members \[52, 53\].](#) In addition to heat transfer mechanisms, forcing functions, boundary conditions, initial state and temperature-dependent varying thermophysical properties of involved materials, the formulated thermal model lays the groundwork for a reliable prediction of:

(a) phase transitions (melting and gasification as vaporization initiates) and decomposition process of heated thermoplastic materials set to elevated temperatures, such as the combustible thermal insulation layer (EPS) placed in the core of the encased precast concrete sandwich arrangement, (b) inception of radiant heat flux between both opposed concrete wythe surfaces of the precast panel system, in the vicinity of the generated air gap, as a consequence of a progressive thermal degradation of the core insulation, subjected to elevated temperatures and (c) transition failure mechanism of the precast wall render, due to interdependencies of the intimate contact between the cement-based render layer (cement mortar) and the combustible thermal insulation layer (EPS), under the intense impact of a fire threat. In other words, the presented modelling technique is well suited to mirror the physical problem and copes with thermal processes directly related to the responsiveness of both insulation layers, as well as the detachment and collapse of attached cement render to insulation.

Although the main stress of the current study is to unfold the fire resistance of the evolved precast system, confirmation of the above results by means of an experimental evaluation (laboratory testing of samples) is also provided as part of a holistic approach aiming to tackle the severeness of this evocative thermal attack. The main procedure aiming to identify temperature deviations and precision between experimental findings of tested specimens and numerical predictions, by virtue of the thermal model, is delineated in the bottom line.

2. Methodology

2.1. Justification of buildings' fire safety in terms of fire resistance criteria

For both structural and supporting elements, the main failure reasons when exposed to fire conditions are directly related to the stability, insulation, and maintenance of their loadbearing capacity (integrity) [54]. Depending on the type of construction, several criteria must be satisfied namely, stability (R), integrity (E) and insulation or temperature rise (I), Fig. 1. The fire resistance rating of a construction product is defined as being the time to failure (from 15 min to 360 min) under a standard fire test when one or more failure criteria apply. The objective of evaluating fire resistance is to unveil the overall behaviour of a building element or system, under a heating pressure and loading state. Experimental observations deliver a means of quantifying the potential of building structures to endure exposure to such kind of severe stresses.

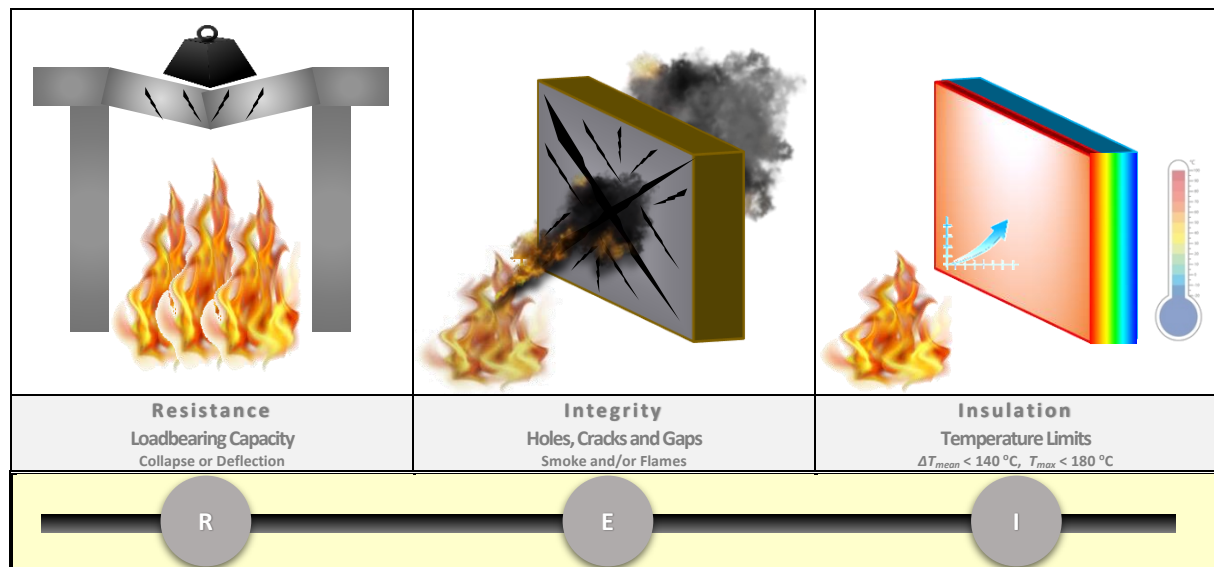


Figure 1. Fire resistance criteria (R, E, I) of building components, from a passive design perspective.

Present fire resistance prescriptive practices [55] date back to the 1920s when Ingberg performed his pioneering full-scale fire tests [56], adopting for the first time a method for evaluating the overall fire severity. As a result of this work, fire codes and design approaches started to get truly related to realistic combustible loads, based on the contents, and use of each room or building. In the late 1960s and 1970s, several experimental and theoretical studies were carried out to develop design methods for structural elements. Standard fire resistance tests of systems or wall assemblies are conducted under rigorously controlled furnace conditions, using gaseous fuel

burners to reproduce the ISO834 temperature-time curve [45]. The increasing interest in modular construction has stimulated several studies focusing on the behaviour of precast concrete wall elements when exposed to a standard fire resistance test [57]. Nevertheless, full-furnace scale tests are expensive, require considerable resources and may prove restrictive when a more in-depth analysis of various parameters influencing the phenomena is required.

An alternative to such an approach is numerical analysis [58]. Recently, aiming to significantly reduce the computational cost, machine learning is used to evaluate stability, integrity, and insulation criteria [49, 59-61]. The increasing trend of developing and implementing performance-based fire safety codes necessitates the use of dedicated fire simulation tools that can be used in a wide field of applications related to building fire safety. Within this framework, the present work aims to clarify the fire resistance capacity of innovative precast concrete wall systems and assess the influence of the fire action by performing a dynamic thermal analysis modelling.

2.2. Fundamental mechanisms of heat transfer through a precast concrete sandwich panel

Within the context of the present dynamic thermal analysis, it is important to identify and clarify heat transfer processes through a precast concrete sandwich panel subjected to a fire scenario, analogous to the one to be examined in this work. As can be seen in Fig. 2, the generic outline of the analysed precast system refers to a sandwich panel of rectangular shape, consisting of two interconnected concrete wythes joined with a carbon steel tubing grid at their lateral boundaries (perimeter). Furthermore, aiming to improve the assembly's thermal efficiency two combustible thermal insulation layers are integrated. A first thermal insulation layer is encased at the core of the precast assembly (between both adjacent concrete wythes), while a second one is placed on one-side of the developed system. Something else to keep in mind, is the locality of fire that affects the direction of heat flow (heat wave propagation), caused by elevated temperatures, through the precast design. Thus, it is requisite to highlight two possible cases of fire evolution that contradictorily affect the time series of degradation (Fig. 2), with respect to both insulation layers:

- **Case A:** The one-side thermal insulation layer is directly exposed to fire. A decomposition process of the one-side insulation layer in front of the thermal attack is shown in a first stage (Phase 1, time point $t_{A,1}$), while the core insulation layer is vaporised in a second stage (Phase 2, time point $t_{A,2}$).
- **Case B:** The one-side thermal insulation layer is not directly exposed to the action of fire. A decomposition process of the core insulation layer is firstly presented (Phase 1, time point $t_{B,1}$), while the one-side insulation layer on the back side of the panel is secondly gasified (Phase 2, time point $t_{B,2}$).

As seen in Fig. 2, both scenarios substantially modify the dynamics of this transient thermal problem. The relevant heat transfer mechanisms from the warmer towards the coolest sides of the panel subjected to fire are as follows [62, 63]:

- Conduction through non-combustible solid sections of the precast design (concrete wythes, and steel tubing), over the entire simulation time.
- Conduction through combustible solid sections of the precast design (both thermal insulation layers), until their complete degradation (melting and gasification).
- Free convection within closed air cavities of steel tubing.
- Long-wave radiation through closed air cavity surfaces of steel tubing.
- Free convection between both concrete wythes, after the degradation of the core insulation layer that generates an air cavity.
- Long-wave radiation among both concrete wythe surfaces and steel tubing segments in contact with the core insulation, after its degradation that generates an air cavity.
- Convection and radiation simultaneously on the side of the exposed precast panel surface to fire.
- Coupled convective and radiative heat transfer in the vicinity of the non-exposed precast panel surface to the surrounding environment.

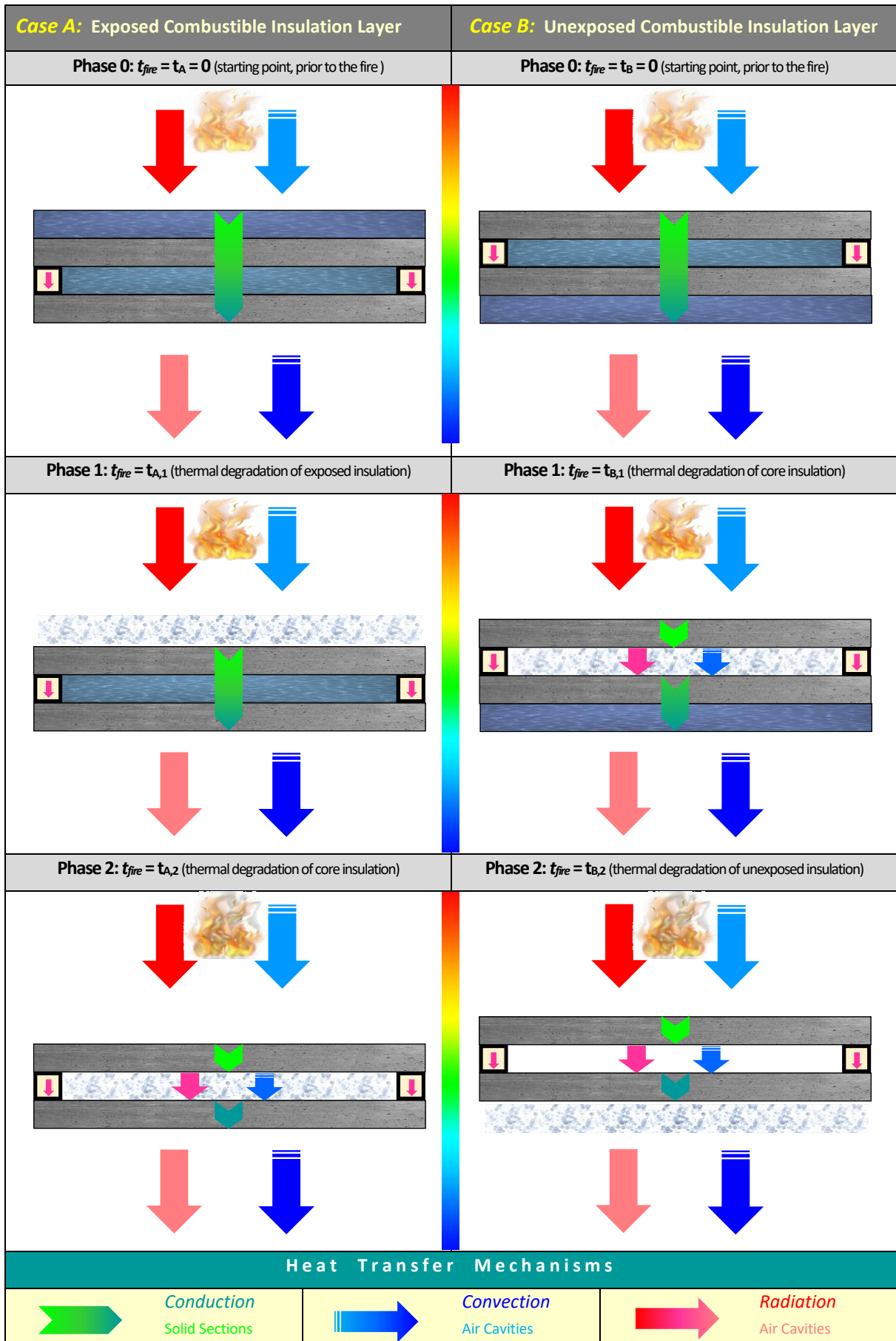


Figure 2. Outline of heat transfer mechanisms, with respect to the examined precast concrete sandwich panel subjected to a fire threat.

The mathematical model, Equation 1, that has been formulated consists of partial differential equations for 3-D heat transfer using Fourier's law [64]. At the beginning of the simulation, ambient conditions ($T_{amb} = 293.15$ K) and constant material thermal properties are assumed, also no energy is generated within the panels' volume. Equation 2 is used as boundary condition to both sides of the panel prior to fire, Phase 0; also, both convection and radiative heat transfer mechanisms are taken into consideration for the calculation of heat flux [64].

$$\frac{\partial^2 T}{\partial x^2} + \frac{\partial^2 T}{\partial y^2} + \frac{\partial^2 T}{\partial z^2} + Q_{gen} = \frac{\lambda}{\rho \cdot C_p} \cdot \frac{\partial T}{\partial t} \quad (1)$$

$$q = q_{conv} + q_{rad} = h_{amb,conv} \cdot (T_{amb} - T_{surf}) + \varepsilon_{surf} \cdot \sigma \cdot (T_{amb}^4 - T_{surf}^4) \quad (2)$$

2.2.1. Heat transfer boundary condition of an exposed to fire precast concrete sandwich panel

When fire initiates, the thermal action in the vicinity of the exposed surface is driven from both convection and radiation and boundary conditions applied in the exposed side are shown in Equation 3 [62]. Heat flux due to convection, $q_{exp,conv}$, in the face of a building element exposed to fire, can be expressed as shown in Equation 4 [50]. It must be noted that in EN1991-1-2 the convective heat transfer coefficient on the exposed to fire surface receives a value of $h_{exp,conv} = 25$ W/(m²·K) [50]. Heat flux due to radiation $q_{exp,rad}$, in the area of a building element exposed to fire, can be as shown in Equation 5 [50]. The view factor φ is a geometrical factor, ranging from 0 to 1, which is related to the extent that the fire front strikes the field of view looking from the building element toward the flame [43]. A value of 1 implies that the entire field of view of the fire enclosure alludes to fire flames or gasses, while a value of 0 suggests that the fire front is completely out of view. To consider a worst-case scenario, the view factor for both cases is set to unity [50]. It is worth mentioning that in case of fully fire-engulfed building elements the effective radiative temperature may be calculated by applying the gas temperature around the examined building elements ($T_{fire,rad} = T_{fire}$).

$$q_{exp,total} = q_{exp,conv} + q_{exp,rad} \quad (3)$$

$$q_{exp,conv} = h_{exp,conv} \cdot (T_{fire} - T_{exp,surf}) \quad (4)$$

$$q_{exp,rad} = \varphi \cdot \varepsilon_{fire} \cdot \varepsilon_{surf} \cdot \sigma \cdot (T_{fire,rad}^4 - T_{exp,surf}^4) \quad (5)$$

2.2.2. Heat transfer boundary condition of a non-exposed to fire precast concrete sandwich panel

Similarly, the relevant thermal action of a non-exposed to fire precast concrete sandwich panel induces simultaneously conjugate heat transfer due to convection and radiation $q_{unexp,total}$ [50]. In this context, the whole heat flux on the non-exposed surface of an element to fire can be defined as indicated in Equation 6. Heat flux due to convection, $q_{unexp,conv}$ in the area of a building element unexposed to fire, can be expressed as shown in Equation 7 [50]. As given in EN1991-1-2 the convective heat transfer coefficient on the non-exposed to fire surface receives a value of $h_{unexp,conv} = 4$ W/(m²·K) [50]. Heat flux due to radiation $q_{unexp,rad}$, at the vicinity of the panel's non-exposed to fire side, can be accounted by Equation 8. It should be noted that for simplicity reasons the effective radiation temperature may be calculated by applying the air temperature around the studied building elements ($T_{amb,rad} = T_{amb} = 293.15$ K).

$$q_{unexp,total} = q_{unexp,conv} + q_{unexp,rad} \quad (6)$$

$$q_{unexp,conv} = h_{unexp,conv} \cdot (T_{amb} - T_{unexp,surf}) \quad (7)$$

$$q_{unexp,rad} = \varepsilon_{amb} \cdot \varepsilon_{surf} \cdot \sigma \cdot (T_{amb,rad}^4 - T_{unexp,surf}^4) \quad (8)$$

Nevertheless, heat flux in this margin is less profound compared to the exposed to fire boundary condition. Therefore, simplifications of the overall ability to consider heat transfer coefficients by both convection and radiation can be applied. Instead of Equations 7 and 8 a less elaborate procedure can be adopted by assuming an equivalent heat transfer coefficient due to combined convection and radiation, $h_{unexp,conv+rad} = 9$ W/(m²·K) [50]. Hence, the entire heat flow on the non-exposed surface to fire can be evaluated by applying Equation 9.

$$q_{unexp,total} = q_{unexp,conv+rad} = h_{unexp,conv+rad} \cdot (T_{amb} - T_{unexp,surf}) \quad (9)$$

2.2.3. Nominal temperature-time curves

Aiming to ascertain the level of fire resistance of a building element the nominal temperature-time curves designated in Eurocode 1 (EN1991-1-2) are applied in the current analysis [50]. The Standard Temperature Time curve is often referred to as the cellulosic curve; in practice, combustible materials in building configurations may be of various forms, besides cellulosic materials to represent a fully developed or post-flashover fire. This Standard Temperature Time curve, Equation 10, also abbreviated as ISO 834, is widely used for fire testing and classification, as well as for fire design of structures for both loadbearing and non-loadbearing elements. As may be seen in Fig. 3(a), the time-temperatures evolution within a compartment for the Standard fire curve constantly grows, evincing a logarithmic trend. In that respect, excessive heat caused by a poor heat dissipation leads to elevated temperatures (maximum temperatures can reach up to 1200 °C, approximately).

$$T_{fire}(t) = 293.15 + 345 \cdot \log_{10}(8 \cdot t/60 + 1) \quad (10)$$

When the external members of a structure exposed to fire, the External fire curve must be used instead. In Eurocode EN1991-1-2 [50], this scenario is catered for by Equation 11. As envisaged, the temperature of fire gases for the External fire curve in Fig. 3(b) show a gradual increase. The prevailing temperature values for this case are mostly lower compared to the Standard fire curve (approximately 265 °C lower, after 1 hour). This can be ascertained, as the temperature curve deemed that fire gases and flames are cooled by the presence of airflow in the ambient environment; thus, this condition reflects the fact that external fire incidents affect less severely enclosed spaces, since they vent to the outdoor environment.

$$T_{fire}(t) = 293.15 + 660 \cdot (1 - 0.687 \cdot e^{-0.32 \cdot t/60} - 0.313 \cdot e^{-3.80 \cdot t/60}) \quad (11)$$

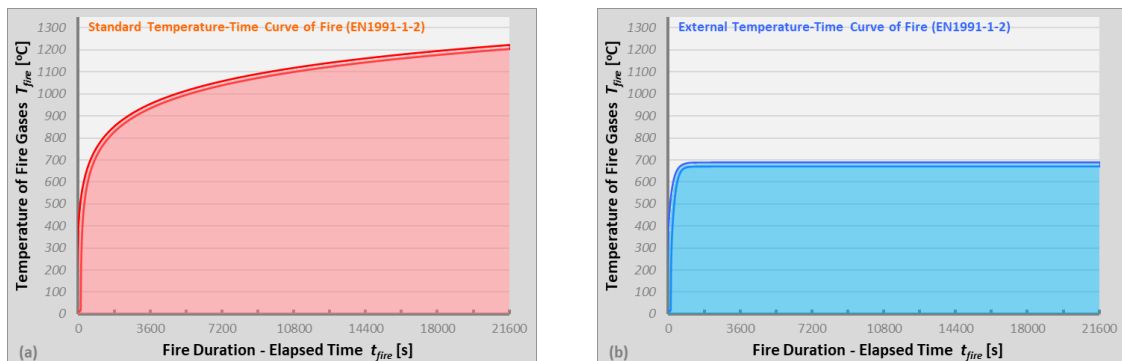


Figure 3. Analysed nominal temperature-time curves indicated in Eurocode 1 (EN1991-1-2): (a) Standard fire curve; (b) External fire curve.

2.3. Analysed precast concrete sandwich panel system

2.3.1. Outline and variations of developed sandwich panel system

Within the framework of this work, an innovative precast concrete sandwich panel has been developed by considering the underpinning principles of preconstruction. These principles are based on the experience of similar efforts and can be viewed as a kind of “proven practices of the past”. However, the extant literature remains vague about the apparent effectiveness of preconstruction under elevated temperatures, which arises from the complexity of such kind of element solutions, and what can be considered suitable for the induced thermal expansion due to fire in the building construction [39-48].

At the same time, there are rising expectations as to what precast design can succeed and how this can be supported by policy measures. It is noteworthy to mention that insulated precast concrete sandwich panels offer tangible benefits over other conventional cladding typologies, deriving from their inherent durability and thermal performance. For this reason, emphasis is placed not on the mechanical and the thermal performance of the arranged system, but rather on conceptual understanding and interpretation of fire defensiveness, as well as on elucidating thermal insulation from a quantitative point of view.

In this study, the analysed preconstructed module is primarily intended to be implemented in residential buildings with a continuous or more rarely intermittent use, referring to detached or semi-detached arrangements, in low to mid-rise and low to mid-density built-up areas. Aiming to evaluate the appropriateness

of a precast system in terms of fire performance, an independent underlying factor of importance is to delineate the general layout of its arrangement. This strong association between fire evolution and both geometry and properties of material layers, favours the necessity to shed additional light in areas related with the layout of the developed precast element, as well as variations of their assembly based on thermal insulation demands.

The general outline of the developed precast system comprises a composite sandwich panel of rectangular shape (700 mm x 700 mm) encompassing two lightly reinforced concrete wythes (C25/30) that embed a combustible thermal insulation layer (EPS) at their core [65]. The thickness of each wythe, as well as the thickness of the insulation encasement filling the cavity, correspond to 50 mm. From a structural perspective, two vertical steel struts (columns) mostly joined by an inclined steel strut are used to link both adjacent concrete layers and ensure structural performance of the precast system. Both vertical struts are placed on the left and right edges of the panel element, while the inclined strut penetrates within the formed cavity, between both interconnected concrete wythes, and splits up the encased thermal insulation layer in two right-triangular sections. The steel strut profiles of the applied coupling system correspond to square hollow structural sections (HSS carbon steel tubing profiles of dimension, 50 mm x 50 mm and a thickness of 3.0 mm, S235). It should also be noted that preconstructed elements are interconnected and connected to major steel loadbearing components of the building structure with custom-designed anchors. A layout of the prototype precast concrete sandwich panel is illustrated in Fig. 4.

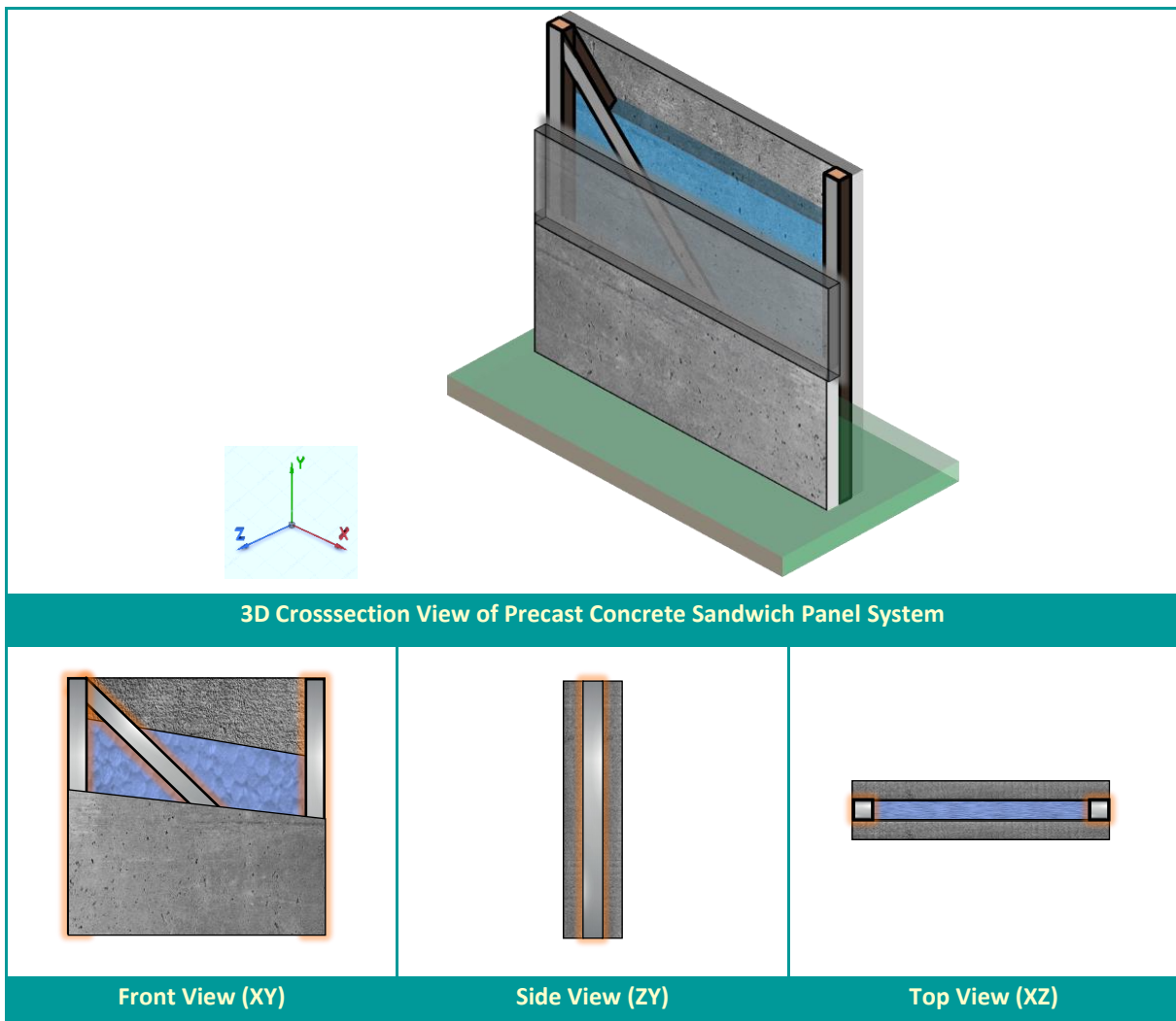


Figure 4. General layout and views of the developed precast concrete sandwich panel system.

Although our initial decision was to not delve into the consequences and impact of varying degrees of heat insulation in relation to the thermal performance of the proposed precast panel, we still *oversee* the fire behaviour of this system that stems from adaptations and inequalities of its assembly. As such, it is prudent to avoid trying to establish accuracy thresholds without assessing the fire performance of the precast system, with varying extents of thermal insulation. Having the above in mind, in addition to the aforementioned outline of the

sandwich panel with an insulation layer filling the gap between both concrete wythes, we have to accommodate more strict demands of precast design in terms of heat stability, while at the same time avoiding potential pitfalls arising by linear thermal bridges within the precast system heat transfer context; on this last point, thermal bridges are widely identified in the vicinity of structural members (struts), as they interrupt the installation and extent of insulation in the cavity [66]. To address this issue of an apparently limited thermal resistance, one must turn to what is probably the most quoted of all arguments in support of thermal efficiency. In that respect, a second thermal insulation layer placed on one-side of the developed module is nominated to tackle this issue and meet challenges derived by policies. In this context and as can be seen in Fig. 5, the analysed precast concrete sandwich panel variations correspond to non-loadbearing wall elements, ranging from basic precast design configurations with an insulation layer placed between both wythes ($d_{EPS-core} = 5$ cm) to more advanced and complicated technical solutions with an additional insulation layer of varying thickness installed on one-side of their assembly (in a range of $d_{EPS} = 2$ cm to $d_{EPS} = 10$ cm, in steps of 2 cm). It is important to stress that for the purposes of this work both exposed and non-exposed placements of the one-side thermal insulation layer to the fire threat are investigated (Case A and Case B, as mentioned before). In all of the cases and within the scope of the present study, both faces of the preconstructed module are covered-coated with a single layer of cement-based rendering mortar (CbM); the thickness of each cement-based mortar lining is consistently taken equal to 1 cm.

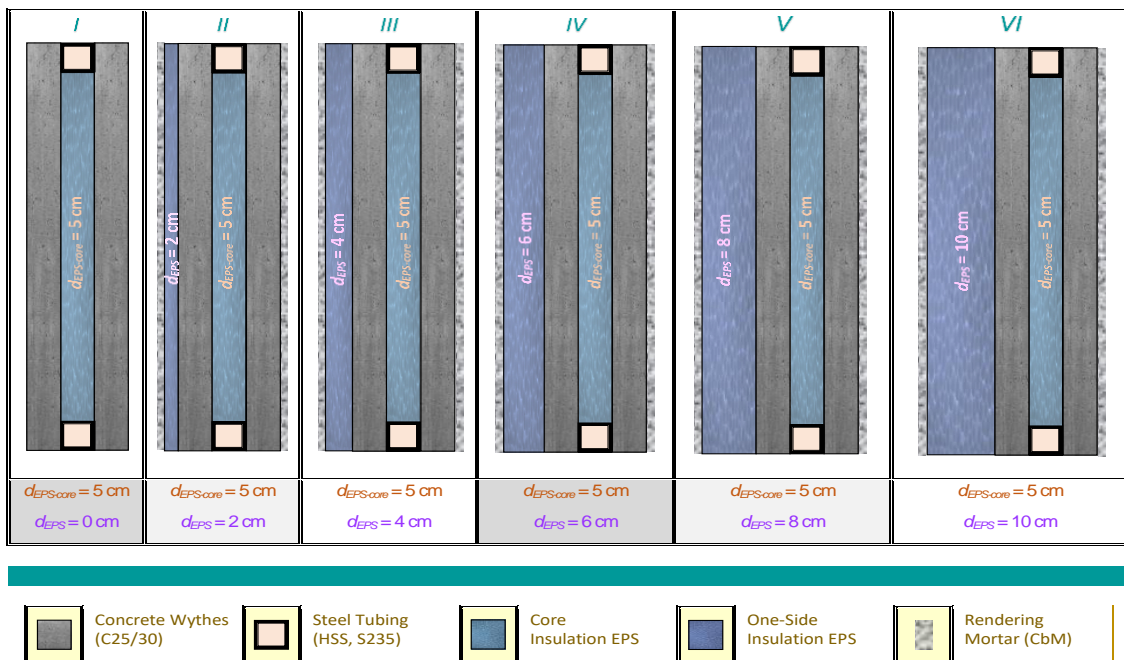


Figure 5. Horizontal cross-sections of precast concrete sandwich panel system (XZ view), with a varying thickness of the one-side insulation layer (d_{EPS}).

2.3.2. Thermophysical properties of involved materials under conventional conditions

Fire resistance performance is mostly identified as a crucial factor to overcome, in designing precast concrete sandwich panels capable to support building applications. In that vein, fireproofing heavily relies on the thermal resistance and capacitance of affiliated materials. According to this exigency, fire engineers should yield high priorities to, among others, passive measures and thermophysical properties of applied materials, such as thermal conductivity λ , bulk density ρ and specific heat capacity C_p . These attributes affect undeniably heat transfer processes, as well as the thermal inertia of building components exposed to a rapidly varying temperature field, such as that can be evinced during a fire strike. Alongside this event, the severity of a thermal attack can be vastly strengthened due to heat transfer processes, such as convection and radiation, within air cavities of precast design. On that account, thermal emissivity coefficient values ϵ of cavity surfaces of the system play a leading role.

In view of this, one should be aware about these aspects, that shed light on fire resistance criteria, and take enforcement actions against those that fall below a certain level. The thermophysical properties of the implicated materials of the system, under an unvarying temperature domain ($T_{amb} = 20$ °C), are listed in Table 1 [67, 68].

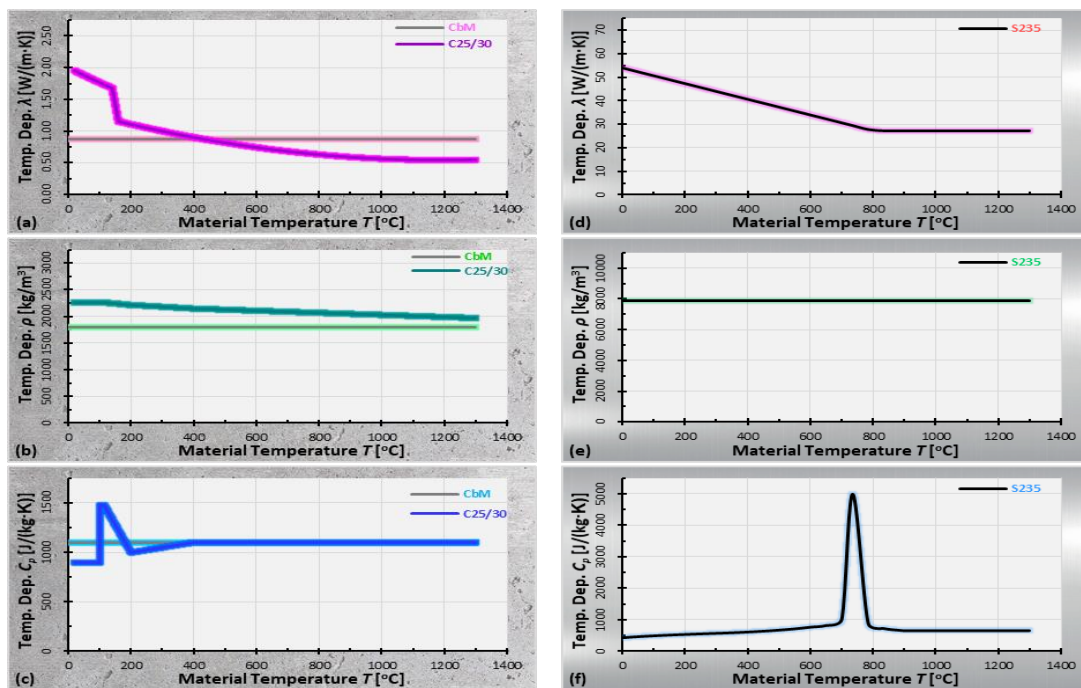
Table 1. Thermophysical properties of concerned materials subjected to a conventional and steady-state of temperature variations (20 °C).

Materials	λ [W/(m·K)]	ρ [kg/m ³]	C_p [J/(kg·K)]	ϵ [-]
Structural Wythes on both Exterior/Interior Surfaces Lightly Reinforced Concrete (C25/30), with $u = 1.5\%$	1.9500	2265.50	900.00	0.70
Coupling System via Carbon Steel Strut Profiles Steel Square Hollow Structural Sections (HSS, S235)	54.0000	7850.00	425.00	0.70
Thermal Insulation in the Core & on One-Side Surface Expanded Polystyrene (EPS)	0.0345	34.00	1280.00	-
Rendering on both Exterior/Interior Surfaces Cement-Based Mortar (CbM)	0.8700	1800.00	1100.00	0.70

2.3.3. Modelling procedure as regards temperature-dependent properties of materials

When analysing the transient thermal performance of a building component exposed to a fire threat, it is highly important to take into consideration the varying properties of involved materials (due to the differentiation of the developing temperature fields), as well as phase change and thermochemical conversion processes of solid materials. The ground of understanding and awareness regarding physical and chemical transformations must be founded by a cautious examination of prior knowledge. Against this background, the deterioration and failure damage of a precast element induced by elevated temperatures should be thoroughly analysed.

At the outset, a swift rise of the temperature field can decisively transform the thermal defensiveness of a wide array of non-combustible building materials. In this regard, the thermal behaviour of such materials relies on thermal conductivity variations as a function of temperature $\lambda(T)$. Under a conventional temperature field these $\lambda(T)$ variations are moderate or almost negligible. In the present investigation, as far as we are concerned this fact is prominently broad, as our main intention is to assess the responsiveness of a precast system against a vicious thermal attack referring to fire. Yet, some additional properties, such as bulk density ρ and specific heat capacity C_p may also be affected or remain invariant under temperature elevation. Therefore, it is essential to initiate by tailoring the onset thermophysical property variations of involved materials according to the dynamic temperature distribution. Temperature-dependent thermophysical properties of composite materials, such as reinforced concrete, cement-based mortar, and structural carbon steel are depicted in Fig. 6 [68-70].

**Figure 6.** Modelling of temperature-dependent thermophysical properties of non-combustible materials (C25/30, CbM and S235).

Secondly, in an effort to avoid drawbacks narrowing the field of application of precast design someone should be aware that the thermal responsiveness of combustible materials can affect dramatically heat transfer mechanisms through the volume of sandwich panel systems. In this context, temperature-dependent

thermophysical properties of such kind of building materials due to physical and chemical processes accentuate an immensely challenging problem. In particular, phase change during the melting-gasification process and, furthermore, decomposition-combustion of heated-burnt materials exposed to an adverse temperature environment, epitomise a transient thermal analysis of high complexity. It is also envisaged that an earlier and more visible development of temperatures can give rise to even more severe thermal stresses, with a direct impact on physical properties of combustible materials. In this study, both examined thermal insulation layers bear upon a combustible thermoplastic material (EPS) that can be affected by a thermal hazard. The thermophysical properties of EPS are almost steady up to 100 °C but thereafter the material enters into a glass transition phase. In a general sense, above 110 °C EPS undergoes a swift thermal degradation. Inflated EPS beads lose their volume and at 150 °C reach up to their initial shape and diameter. Moreover, at approximately 150 °C EPS is turned to a viscous liquid and can no longer be classified as a solid insulating layer. Beyond 278 °C, EPS experiences a transition of its phase as vaporization initiates [71-80]. With that knowledge in mind, and while striving to realise a successful thermal analysis, this study follows a formulation plan under the lens of a discrete modelling procedure for both insulation layers. Thus, we are inferring that by passing distinct thermophysical properties to each slot of insulation (Fig. 7) someone can iteratively emulate the actual processes of heat through the analysed system, while still preserving the initial layout of the developed model. To summarise, our modelling technique relies on a discrete notion of possible EPS placements, as follows:

- **Placement A [EPS at the core of the module]:** For a range of temperature variations within 20 °C to 100 °C the thermal conductivity of EPS at the core of the sandwich system is approximately $\lambda_{EPS-core(20^{\circ}C-100^{\circ}C)} \approx 0.035$ W/(m·K). A further increase of temperatures, from 100 °C to 150 °C, results in an almost linear increase of thermal conductivity; hence, it is $\lambda_{EPS-core(150^{\circ}C)} \approx 0.200$ W/(m·K). On the other side, bulk density ρ and specific heat capacity C_p maintain a constant value at the temperature range of 20 °C to 150 °C. Beyond this limit, as already specified, liquification, vaporization and thermal decomposition processes of the combustible thermal insulation layer become visible. Furthermore, for temperatures above 150 °C, and as EPS is in a vapour state, we consider that the thermophysical properties of this generated cavity between both concrete wythes corresponds to a still air layer. The aforementioned modelling tactic to cope with the shown physical processes is illustrated in Fig. 7(a)-(c).
- **Placement B [EPS on one-side of the module]:** For a temperature up to 150 °C, the same trend applies as before ($\lambda_{EPS-T<150^{\circ}C} = \lambda_{EPS-core(T<150^{\circ}C)}$). Then again, when the temperature exceeds this critical point and due to computation limitations of the modelling formulation, the thermal conductivity λ of EPS on one-side of the panel system receives a rather high value, that corresponds to a negligible thermal resistance. On the contrary, in association with bulk density ρ and specific heat capacity C_p variations of EPS, a reversed approach is embraced; very low values of ρ and C_p , with an almost negligible thermal capacity are taken into account. The above rule somehow assists to simulate the loss of the flammable thermal insulation layer, as in practice EPS is gradually melted and evaporated (transitions between various physical states and downfall of thermal stability). The key stages used for this modelling process are indicated in Fig. 7(d)-(f).

This modelling technique of phase transitions of both EPS layers allows for a coherent and consistent prediction of the heat flux through the examined precast element under the likelihood and the severity of a fire occurrence. In addition, it should be pointed out that a possible ignition of EPS vapours is not contemplated, as it's not part of the extent of this study; thus, when chemical bonds are violated and moulded through a combustion reaction released heat is omitted. In particular, emphasis has been placed on the thermal behaviour based on a certain fire action.

Thirdly, as regards the rendering of the combustible thermal insulation layer, it is important to bear in mind the exhibited transition process of phase change. In that respect, EPS remains in a solid state for temperatures below 150 °C; above this point, EPS turns to a viscous liquid which -as temperature increases- goes through thermal decomposition. This critical temperature regarding the connection between both interfacing layers is a threshold that, when passed, leads to the melting of EPS and the fall of the cement-based mortar (CbM). Due to the abolishment of the intimate contact between both layers under the strike of a fire, flakes of coating are progressively detaching from the precast sandwich panel system.

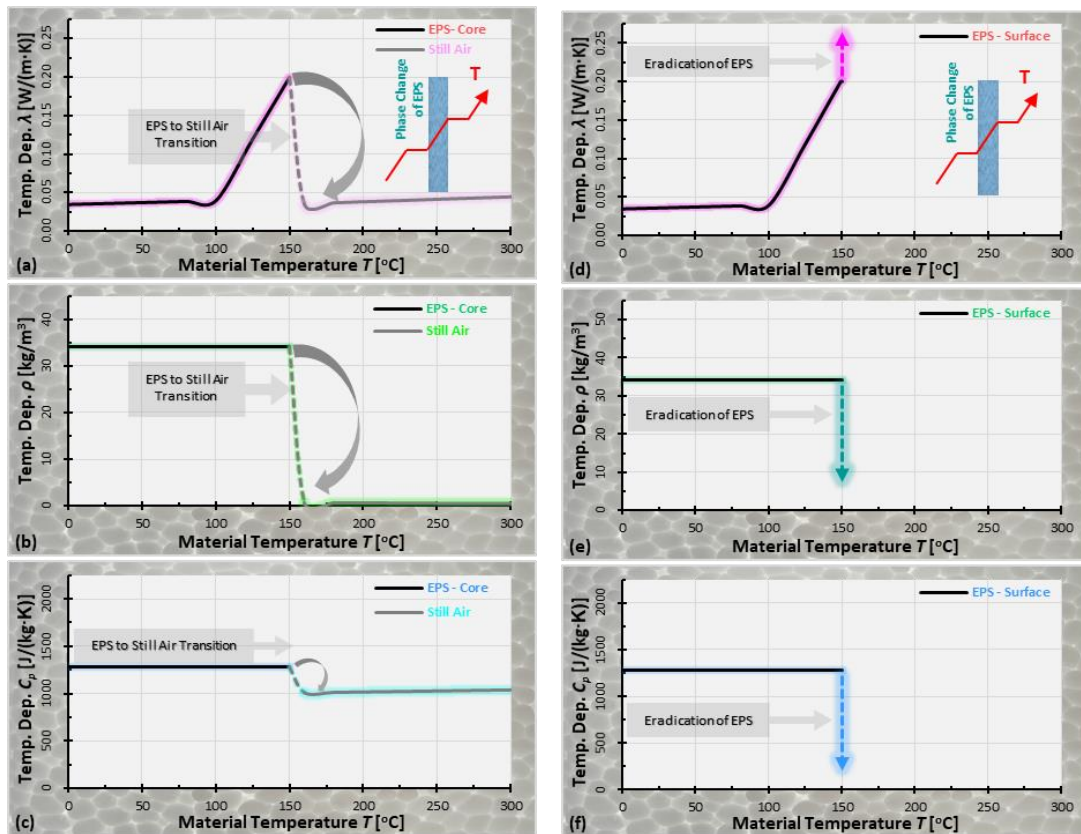


Figure 7. Modelling of temperature-dependent thermophysical properties of combustible material (EPS, for both possible placements).

This latter point bears attention, as it may crucially influence the heat propagation through a building configuration caused by a fire wave. With an eye toward realising an unflinching thermal analysis, it is necessary to discern the point of time at which the interface layer temperature T_{int} upon contact of both layers reaches 150 °C. This tipping point stipulates the time at which the thermal analysis should be adapted to mirror the physical phenomena (up to the point of incipient collapse of CbM, due to the loss of EPS), while taking note of modelling restrictions and numerical limitations. Thereby, someone should put effort in order to eradicate and remove the rendering of the studied system (as CbM falls off). Within the core of this vision, a preliminary transient thermal analysis (exploratory phase over the entire period of the simulation) has been carried out to detect the critical juncture at which the interface layer temperature upon contact of both layers reaches the tipping point (150 °C). The possible events of scenarios, as a function of the insulating render exposure to fire, that could ensue are as follows:

- Scenario A [CbM-to-EPS interface exposed to fire]:** As can be seen in Fig. 8(a), the CbM-EPS interfacial temperature T_{int} exceeds the critical limit in less than five minutes for all configurations of the panel system, with a varying insulation thickness (d_{EPS}) ranging from 2 cm to 10 cm. Likewise, the graphs in Fig. 8(b)-(d) depict the time-dependent variations of the thermophysical properties of the insulating render, with respect to an intense thermal action. To cope with the challenges of this labour, the variations of λ , ρ and C_p in this figure, reflect an approximately zero thermal resistance and thermal capacity of the render. It must be stated that an almost identical trend can be assumed for both considered fire actions (Standard fire curve and External fire curve).
- Scenario B [CbM-to-EPS interface unexposed to fire (reversed fire front)]:** In a similar way, someone can harvest the time-dependent thermophysical properties of the rendering system of insulation, when the latter is found on the unexposed face of the precast element. However, in contrast with Scenario A, where correlations among fire action, one-side insulation thickness, and the critical limit were displayed in a narrow time frame, nothing of the kind arises in this event. This can be attributed to the pivotal role of both concrete wythes, as well as the core insulation that retards the temperature amplification to the interface limit between CbM and EPS. The induced delay mainly relies on how fast temperatures increase on the fire region. A less intense fire action can weaken the severity of heat propagation and consequently restrain the temperature elevation. Then again in a lower degree the insulation thickness also affects the time point of

the render collapse/fall. In this context, failure of the CbM-to-EPS bond occurs after approximately 3 hours (ISO834).

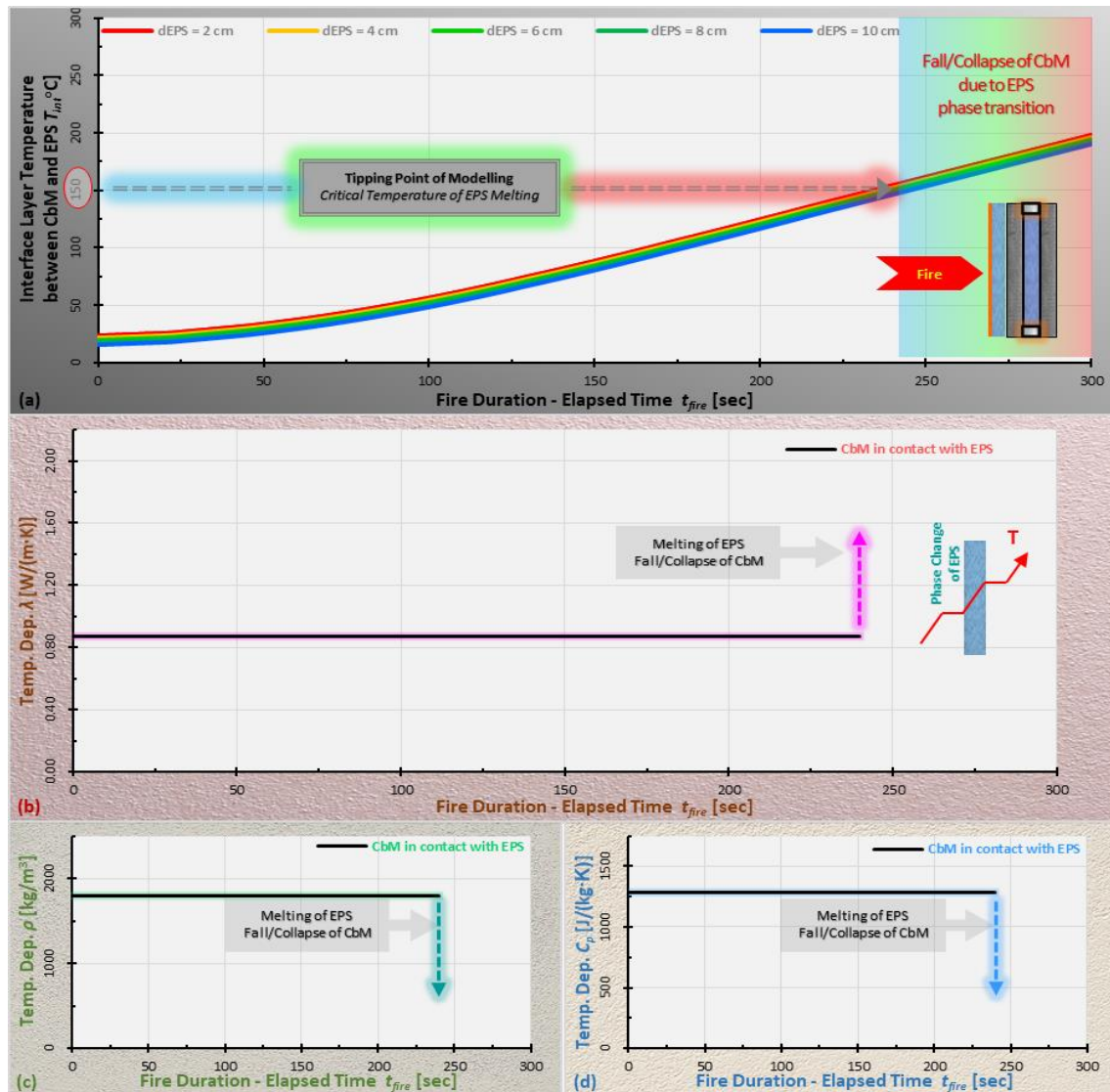


Figure 8. (a) Temperature evolution at the interface upon contact of both layers (CbM and EPS); (b)-(d) Modelling of time dependent thermophysical properties of insulating render, directly exposed to a fire action.

We then focus on the modelling of the optical properties of involved materials to cope with the demands of the solution technique (Fig. 9). Therefore, a rigorous methodology is implemented to predict heat transfer by dint to emission of electromagnetic waves. The transient heat flux due to thermal radiation, at both boundaries of the panel system as well as within air cavities of the carbon steel square hollow structural sections (HSS, S235), is strongly tied to the value of the thermal emissivity ϵ of the involved material surfaces. Against this background, as seen in Figs. 9(a)-(c) the followed procedure takes into account the actual optical properties of most implicated material surfaces. However, the thermal decomposition process of both combustible thermal insulation layers redefines substantially the formulation tactic, since constraints referring to the modelling geometry necessitate an alternative procedure. In this light, a purely conventional and well-known thermal analysis approach has been replaced with an alternative procedure that assumes a fictitious transparent material “occupying” the space of the EPS layer after its destruction; this state of temperature-dependent thermal emissivity variations is displayed in Figs. 9(d)-(f). For the intervals during which the temperature of EPS is below the critical temperature of melting the thermal emissivity of neighbouring solid materials is considered $\epsilon = 0$. But when it comes to deal with EPS in a fluid state, we should deem the actual thermal emissivity values of adjacent solid materials. By following this rational technique, we can steer a path away from a situation in which thermal radiation would be incorrectly neglected. To conclude, as we seek to better understand the response of panel systems under fire threats, it is necessary to introduce rigorous methods adequate to predict heat fluxes and temperature variations.

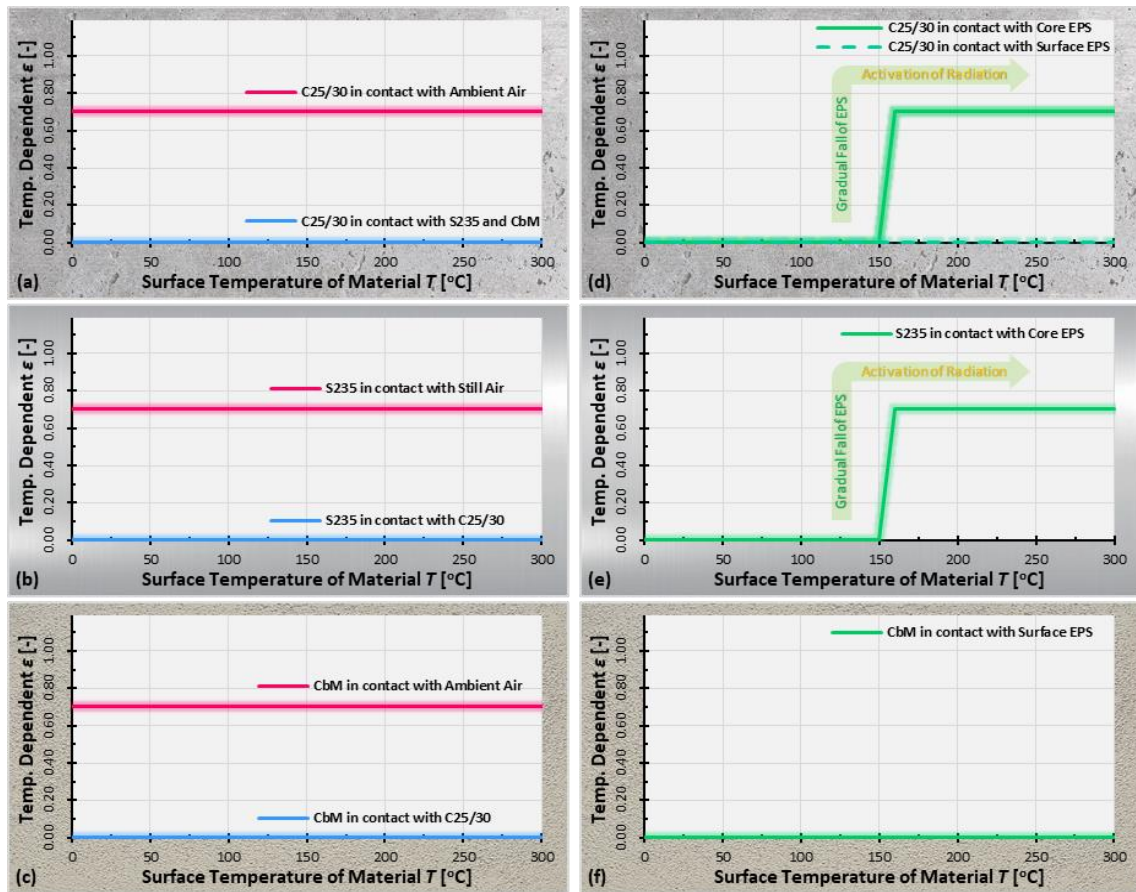


Figure 9. Modelling of temperature-dependent thermal emissivity of basic material surfaces (C25/30, CbM and S235) of the precast system.

2.3.4. Datasets of studied configurations of the sandwich panel system

In the previous subsections a more or less lucid framework was suggested, which underlines the central issues of a holistic procedure to feed in a decent way the algorithm of the actual problem. On this basis, the present work aims to identify and interpret connections between several key aspects of the precast concrete sandwich panel system arrangements with the affiliated evolution of temperatures through their structure, due to the Standard temperature-time curve. This condition furthermore highlights the need to look beyond the margins of a strict forcing function and pay attention to the effects and vulnerability of a less grave forcing function, such as the External temperature-time curve. As reflected in Table 2, a total of twenty-two datasets of cavity wall arrangements were analysed by adopting a numerical technique and more specifically a finite element method (FEM).

Table 2. Datasets of analysed precast system, with respect to investigated parameters.

No. of Case	Type of Fire Action Temperature-Time Curve	Exposure of One-Side Thermal Insulation Layer	Thickness of One-Side EPS Panel, d_{EPS} [cm]
Case A.1.	■ Standard	● Exposed to Fire	----- 2 cm
Case A.2.	■ Standard	● Exposed to Fire	----- 4 cm
Case A.3.	■ Standard	● Exposed to Fire	----- 6 cm
Case A.4.	■ Standard	● Exposed to Fire	----- 8 cm
Case A.5.	■ Standard	● Exposed to Fire	----- 10 cm
Case B.1.	■ Standard	● Exposed to Air	----- 2 cm
Case B.2.	■ Standard	● Exposed to Air	----- 4 cm
Case B.3.	■ Standard	● Exposed to Air	----- 6 cm
Case B.4.	■ Standard	● Exposed to Air	----- 8 cm
Case B.5.	■ Standard	● Exposed to Air	----- 10 cm
Case C.1.	■ Standard	○ No Insulation / No Rendering	----- 0 cm

No. of Case	Type of Fire Action Temperature-Time Curve	Exposure of One-Side Thermal Insulation Layer	Thickness of One-Side EPS Panel, d_{EPS} [cm]
Case A.6.	■ External	● Exposed to Fire	----- 2 cm
Case A.7.	■ External	● Exposed to Fire	----- 4 cm
Case A.8.	■ External	● Exposed to Fire	----- 6 cm
Case A.9.	■ External	● Exposed to Fire	----- 8 cm
Case A.10.	■ External	● Exposed to Fire	----- 10 cm
Case B.6.	■ External	● Exposed to Air	----- 2 cm
Case B.7.	■ External	● Exposed to Air	----- 4 cm
Case B.8.	■ External	● Exposed to Air	----- 6 cm
Case B.9.	■ External	● Exposed to Air	----- 8 cm
Case B.10.	■ External	● Exposed to Air	----- 10 cm
Case C.2.	■ External	○ No Insulation / No Rendering	----- 0 cm

2.4. Numerical technique of the transient thermal analysis and experimental validation of the model

2.4.1. Formulation of Finite Element Analysis by adopting the Finite Element Method

Over the past few years, keen interest has been paid on addressing engineering problems, such as those in connection with heat transfer through building envelopes. The most efficient plan to bring off a rigorous transient thermal analysis of a building element prone to a fire and to attenuate concerns related to structural integrity, is to eradicate the barriers that inhibit the implementation of an exhaustive simulation.

In this work, in order to unveil the eminence of the previously quoted aspects and, moreover, assess temperature variations of precast concrete sandwich panels, a numerical procedure has been sought. In this view, the contemplated computational formulation leans on the utilisation of a Finite Element Analysis (FEA). This inherent approach enables a coherent preparation and clarification of complex problems since building structures can be treated by analogy with electric networks or, equally, as a setup of partial differential equations (PDE) [63].

In an effort to address core issues directly linked to the computational formulation of PDEs, COMSOL Multiphysics® simulation software has been utilised [63]. This highly interactive program delineates an excellent trade-off in terms of straightforwardness, precision, robustness, and computational versatility to a wide array of finite element procedures and transient concerns. Its environment facilitates the development of a model relying on fundamental PDEs mirroring heat transfer mechanisms. Overall, to formulate and resolve a thermal model by means of a Finite Element Method (FEM) it is very important:

- To delineate the kind of the thermal analysis (stationary or time-dependent PDEs solution).
- To designate physical parameters and variables of heat transfer analysis.
- To generate the 3D model geometry of precast concrete sandwich panels (domains).
- To indicate thermophysical properties of involved materials.
- To define boundary conditions on all surfaces of the model (domain edges).
- To define and tailor the finite element mesh of the model.
- To specify the whole length of the thermal analysis and the corresponding time step.

An indicative layout of the analysed precast concrete sandwich panel (geometry of the model) by using COMSOL Multiphysics® under a time-dependent tactic is depicted in Fig. 10. It should be stated that the geometrical characteristics and thermophysical properties of materials, as well as the environmental settings on the limits of the analysed element (forcing functions on both sides of the model and adiabatic surfaces for the rest of its layout), are apparently correlated to the details specified in Section 4. Yet, as can be seen the 3D FEM is meshed and swept by use of a mesh that takes into account different element types and element size features. As the number of mesh elements raises, the precision of calculations is ameliorated, while computational time grows longer. As far as we are concerned, a normal mesh size that underlines a fair precision of simulations has been applied; for the selected degree of freedom of this analysis a reasonable period of time is required, while not

exceeding the processing power of the computing machine. For the aims of this inquiry, the entire length of simulating results was confined at 6 hours.

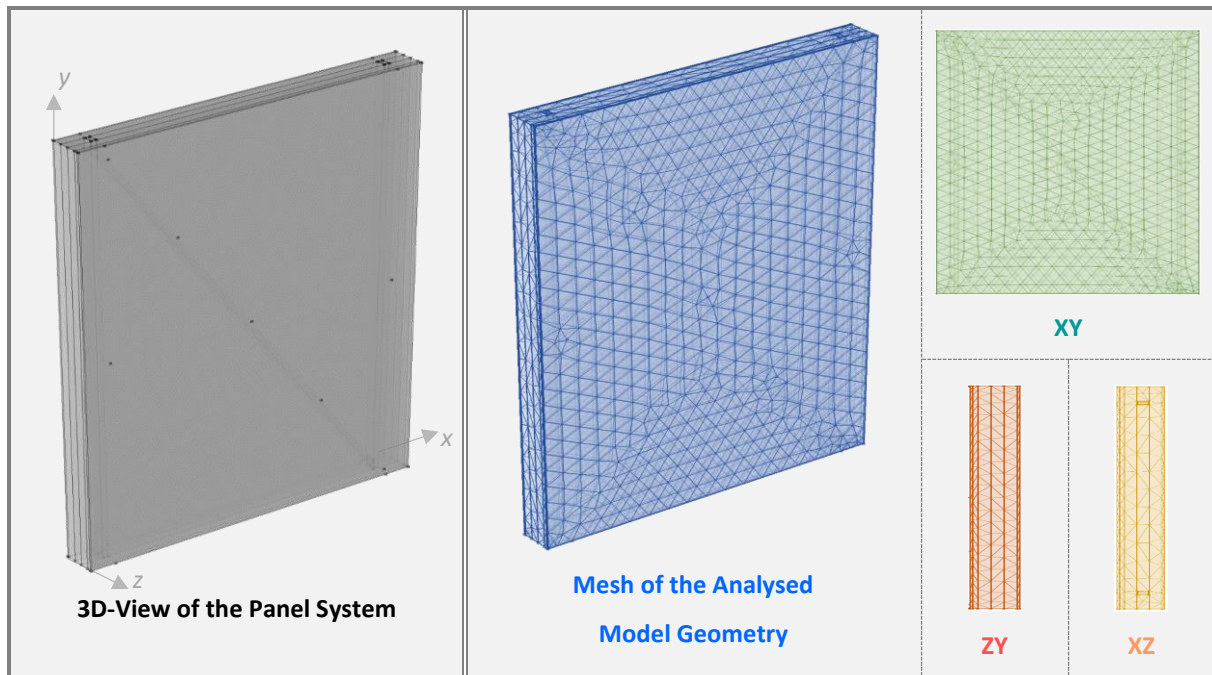


Figure 10. Three-dimensional modelling and meshing arrangement of the thermal probe, reflecting heat transfer processes through a precast concrete sandwich panel system, by using COMSOL Multiphysics® simulation software.

Within this framework, the developed model can predict the temperature series through the examined element, due to a certain temperature increase regime in accordance with the concept of EN1991-1-2 [62]. Inevitably, there are some critical modelling concerns in a FEA aiming to cope with fire dynamics, and borderlines have to be drawn which may allow us to conduct a concrete thermal analysis and attenuate criticism of the modelling technique. In particular, we were also keen to ensure that modelling strictness on the borderlines between insulating rendering (CbM) and thermal insulation on one-side (EPS) did not suffer. In this light, we will outline a time-dependent methodology to tackle this critical issue and acquire knowledge in this field regarding the thermal defensiveness of the system. Overall, this transient methodology relies on a two-step scheme:

- **1st Step [Preliminary Thermal Analysis]:** In an initial phase, numerical simulations are realised to predict the point of incipient collapse of CbM, due to melting of EPS. The conclusion of this step, as indicatively demonstrated in Fig. 8, delimits the time-dependent thermophysical properties of the insulated render.
- **2nd Step [Ultimate Thermal Analysis]:** In a following phase we redefine the solution procedure by feeding new data into the model. Thus, emphasis has been placed on numerical simulations while taking into consideration the time-dependent responsiveness of the insulated rendering system.

2.4.2. Validation of the thermal model by means of a laboratory-based experiment

A medium-scale test was conducted with the aim to assess the fire resistance of the precast element (Case C.1., as per Table 2) and to validate the developed thermal model. The test followed the mandate of EN 1364-1 [81] (for non-loadbearing elements). A three months' old specimen was pre-conditioned carefully in a controlled environment of $20^{\circ}\text{C}\pm 2^{\circ}\text{C}$ and 65% air temperature and relative humidity, respectively. The specimen measuring 700 mm x 700 mm x 150 mm was embedded in a 3.00 m x 3.00 m steel frame lined and filled with refractory and aerated concrete blocks, respectively, as shown in Fig. 11. The frame comprised the shutter of a large vertical fire resistance furnace and also included a second precast element which does not make part of the investigation discussed herein. The specimen of interest was rested on refractory concrete blocks while all other edges were furnished with a rockwool strip so as to allow for free expansion both horizontally and vertically. The exposure time-temperature curve was the ISO 834 one [45] running for a total of 186 min without compromising element's integrity. The temporal evolution of temperature was measured at the middle of the specimen height using four

thermocouples, as indicated in **Fig. 12**: one in the exposed to fire side (TC2; at mid-thickness of the exposed concrete wythe), one in the unexposed side (TC3; at mid-thickness of the unexposed concrete wythe), one on the surface of the unexposed side (concrete wythe) (TC4) and another on the surface of the carbon steel tube (hollow core side) adjacent to the exposed concrete wythe (TC1). For the measurement positions TC2, TC3 and TC4, 2 mm diameter roving thermocouples were used with an accuracy of $\pm 4^\circ\text{C}$. At the unexposed side of the concrete surface, a copper disc thermocouple was used with the same accuracy. All thermocouples and measurement equipment were connected to a data logging system with a sampling frequency of 0.10 Hz.



Figure 11. Experimental configuration of the embedded specimens in a walled metal steel frame in the large-scale furnace (specimen of interest: the one on the left).

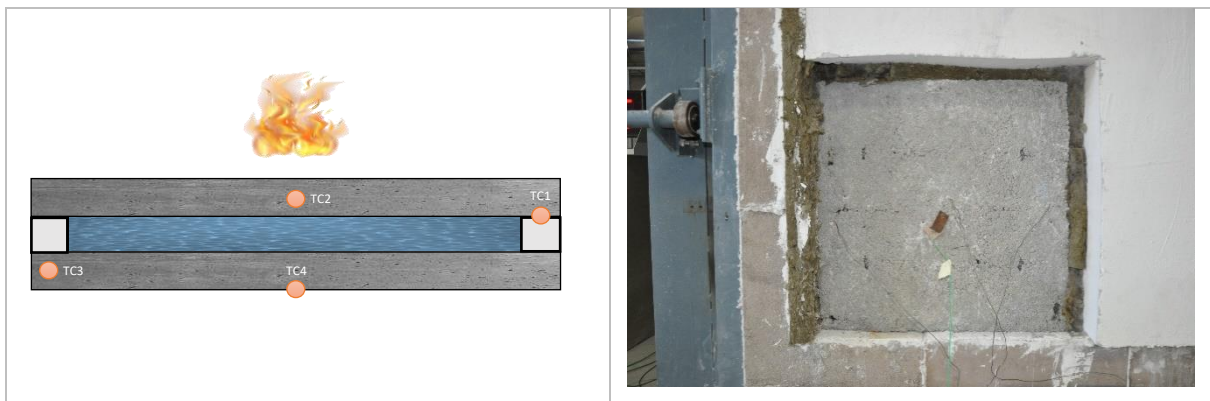


Figure 12. Schematic of the positioning of the thermocouples (left) and positioning of the thermocouples on the unexposed surface of the specimen (right).

In **Fig. 13**, simulation results using the numerical model (Case C.1., as per **Table 2**) are compared to experimental measurements corresponding to the unexposed surface of the specimen (TC4). Good qualitative and quantitative agreement is attained for the predicted temporal evolution of the unexposed surface temperature. Discrepancies between simulation results and experimental measurements are attributed to the modelling assumptions, especially regarding spalling, cracking and dehydration processes occurring in reality (see **Fig. 14**) but not simulated. Additionally, the fact that the readings from a single thermocouple were taken (rather arbitrarily) as representative of the mean unexposed surface temperature introduces yet another reason for measured vs. calculated temperature discrepancies. On the other hand, simulation results of carbon steel tubing, TC3, when compared to the outcomes of the laboratory testing, exhibit a less tolerable agreement. In that respect, the omitted phenomenon of involuntary dehydration, as well as uncertainties under controlled conditions give rise to deviations between numerical and experimental approaches. Nevertheless, there is a qualitative agreement and numerical results seem to capture the overall trend of temperature increase.

A ThermaCAM B4, FLIR thermal camera was settled-positioned in front of the test configuration, to record additional information regarding the thermal response of the unexposed specimen surface. The refresh rate was set at 50 Hz, accuracy was $\pm 2\%$ and repeatability $\pm 1\%$. At last, **Fig. 15** presents thermal imaging of the unexposed surface of the specimen 93 min and 188 min after the start of the experiment.

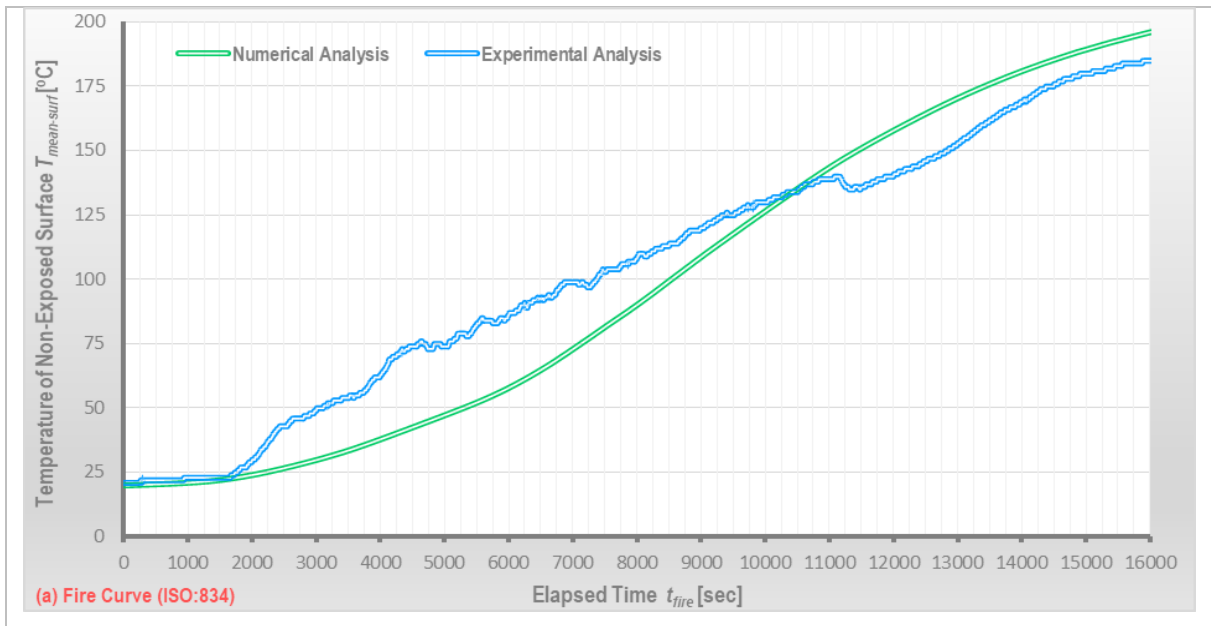


Figure 13. Measurements and model predictions of the temperature of the unexposed surface.



Figure 14. Dehydration (left, as manifested on the specimen placed on the right of the frame) and hairline cracking (right) during the test.

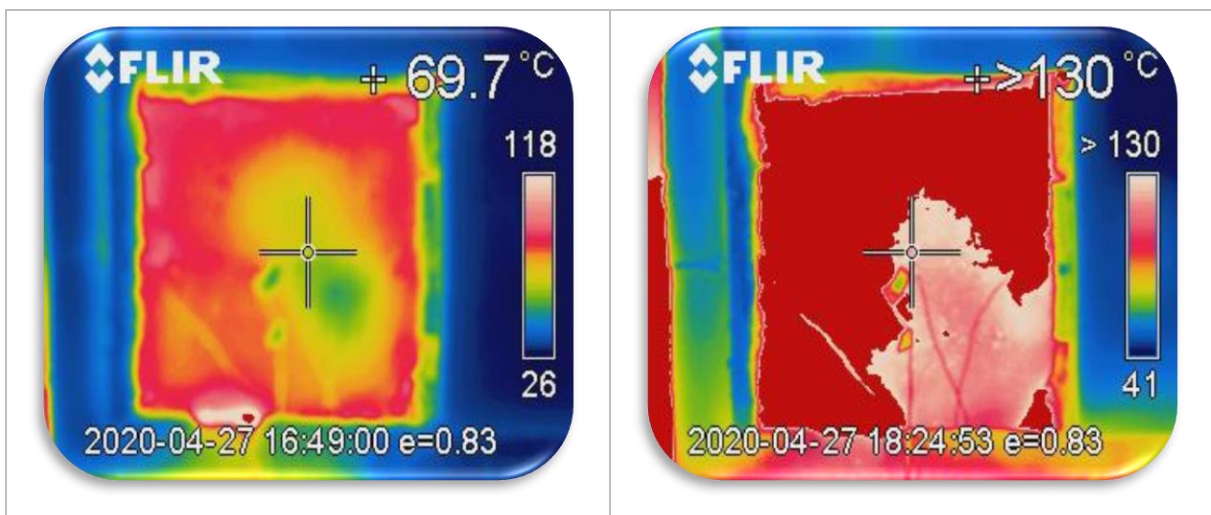


Figure 15. Unexposed surface temperature 93 min (left) and 188 min (right) after fire initiation.

3. Results and discussion

The main concerns raised over the adoption of a transient thermal analysis of a precast concrete sandwich panel system exposed to a thermal attack relate to the attributes of insulation regions in which thermal conduction is reduced while creating a crucial buffer zone (heat barrier). In this regard, the thickness and position of thermal insulation layers can dominantly affect the transient phenomena of heat flow. Besides, someone should bear in mind that the efficacy of this dynamic buffer zone strongly relies on the combustibility of the involved layers. Furthermore, the fall of the rendering system in contact with the combustible layer should be cautiously considered as it may affect the evolution of temperatures.

Bridging these gaps by virtue of a robust and flexible thermal model is essential in terms of fire safety and reliability of building components. In this context, FEA outcomes aiming to deliver a reliable prediction of the transient temperature gradient within the analysed modular system are unfolded in the paragraphs that follow. Along these lines, the Standard fire curve is acknowledged as a benchmark for measuring the thermal defensiveness of the suggested precast assembly. In addition to that, the temperature evolution is also delimited while studying a less grave forcing function, such as the External fire curve.

3.1. Temperature increase on the non-fired side of the analysed sandwich panel system

With a focus on fire dynamics of precast structures embracing high performance modular systems, this section aims to reveal the impact of the one-side surface insulation on the temperature increase of the non-fired side of the analysed sandwich panel system. This system spanning from lowly to highly insulated variations of its primary design is examined for both the Standard and External temperature-time curves. Accordingly, results in Fig. 16 and Fig. 17 draw attention to the mean-surface $T_{mean-surf}$ and the peak-surface $T_{peak-surf}$ temperature variations of the unexposed to fire element of this analysis, respectively.

The plots in Fig. 16(a), referring to a panel system having a one-side insulation exposed to a Standard fire curve (Case A), demonstrate a swift increase of $T_{mean-surf}$ temperatures. In a little bit more than 2 ½ hours the non-fired side of the element reaches up to 100 °C, approximately. Moreover, as can be seen after 3 ¾ hours the $T_{mean-surf}$ temperatures on the unexposed surface of the studied element reach above a certain value of 160 °C, indicating a failure of the insulation criterion (I). The above trend of temperature evolution, as well as observed invulnerability levels based on temperature increase limitations, are almost equivalent for the entire range of the examined assemblies with a varying thickness of the combustible insulation layer d_{EPS} . It is an undeniable fact that as soon as the interface temperature between rendering and insulation reaches up to 150 °C the decomposition of the EPS is realised promptly. This process is adequately supported by a rational approach that allows a concrete modelling of the CbM fall as soon as EPS turns into a liquid phase. Moreover, it is apparent that the elevation rate of temperatures remained significantly lower for the remaining period of this thermal analysis; the conclusion of this transient thermal analysis gives rise to temperatures that almost reach up to 200 °C.

On the other hand, at the nexus of fire performance of the examined system the corresponding temperature evolution graphs in Fig. 16(a), associated to a panel system having a one-side insulation unexposed to a Standard fire curve (Case B), elucidate a quite different development of $T_{mean-surf}$ temperatures. In this light, while for Case A $T_{mean-surf}$ temperatures remain almost steady (approximately 20 °C) for a period less than ½ hour, for Case B corresponding temperatures on the unexposed to fire surface are unvarying during the first 1 ½ hours of the thermal analysis, by virtue of the thermal resistance of both performing insulation layers. Therefore, when the insulation is located on the non-fired side, the rate of thermal transmittance to the unexposed surface is shown to be evidently lower (delayed), at least for a certain period of time, that may evince a safe zone in terms of temperature increase and resilience of building structures. Nevertheless, after a certain period of 1 ½ hours the heat wave caused by the fire attack results to a gradual melting of both insulation layers that in turn eradicates the beneficial effect of this buffer zone. This condition induces a vicious progress of temperatures on the unexposed surface of the studied system. Yet, after approximately 2 hours the non-fired side of the element reaches up to 100 °C, while after a period of 2 ½ hours exhibited temperatures for Case B exceed the ones shown for Case A, as the evolution trend is shown to regain the lost ground. The cross-over of temperature curves cannot be easily interpreted by the position of the one-side insulation and the sequence of degradation/failure of this element, caused by a gradual melting of both insulation layers (see Fig. 2) and a possible fall of the insulating render. However, it is essential to bear in mind that under the given dynamic conditions, the shown balance among thermal resistance and thermal capacity of material layers, can inevitably affect the propagation

of heat through the volume of the element in the time domain [82]. Moreover, the critical temperature of 160 °C is acquired after 3 ¼ hours; at last, it should be mentioned that through the lens of this procedure maximum temperatures marginally exceed 200 °C.

Further aspects of this computational inquiry interpret temperature evolution with the impact of an External fire curve. The above outreach strategy to determine the leaning of temperature evolutions is illustrated in Fig. 16(b). As expected, temperatures are kept lower for a longer period for both examined cases in comparison to those computed for the Standard fire curve case. In this context, a temperature of almost 100 °C on the unexposed surface of the element is succeeded after a period of 4 hours and 3 ½ hours for Case A and Case B, respectively. Then again, the corresponding peak temperatures of the examined system never exceed the critical limit of the insulation criterion, at least for a period of 6 hours which denotes the limits of the present transient analysis; in particular, temperature peaks correspond to 130 °C and 145 °C, for both considered case clusters. It is clear that the External nominal temperature-time curve reflects a less severe state within the mainstream of available fire actions. As regards to the influence of d_{EPS} the simulation findings do not underline a remarkable contribution. On average, temperature deviations among marginal assemblies ($d_{EPS} = 2$ cm and $d_{EPS} = 10$ cm) range up to 5 °C, while maximum differences reach up to 10 °C (for Case B, at $t_{fire} \approx 100$ min).

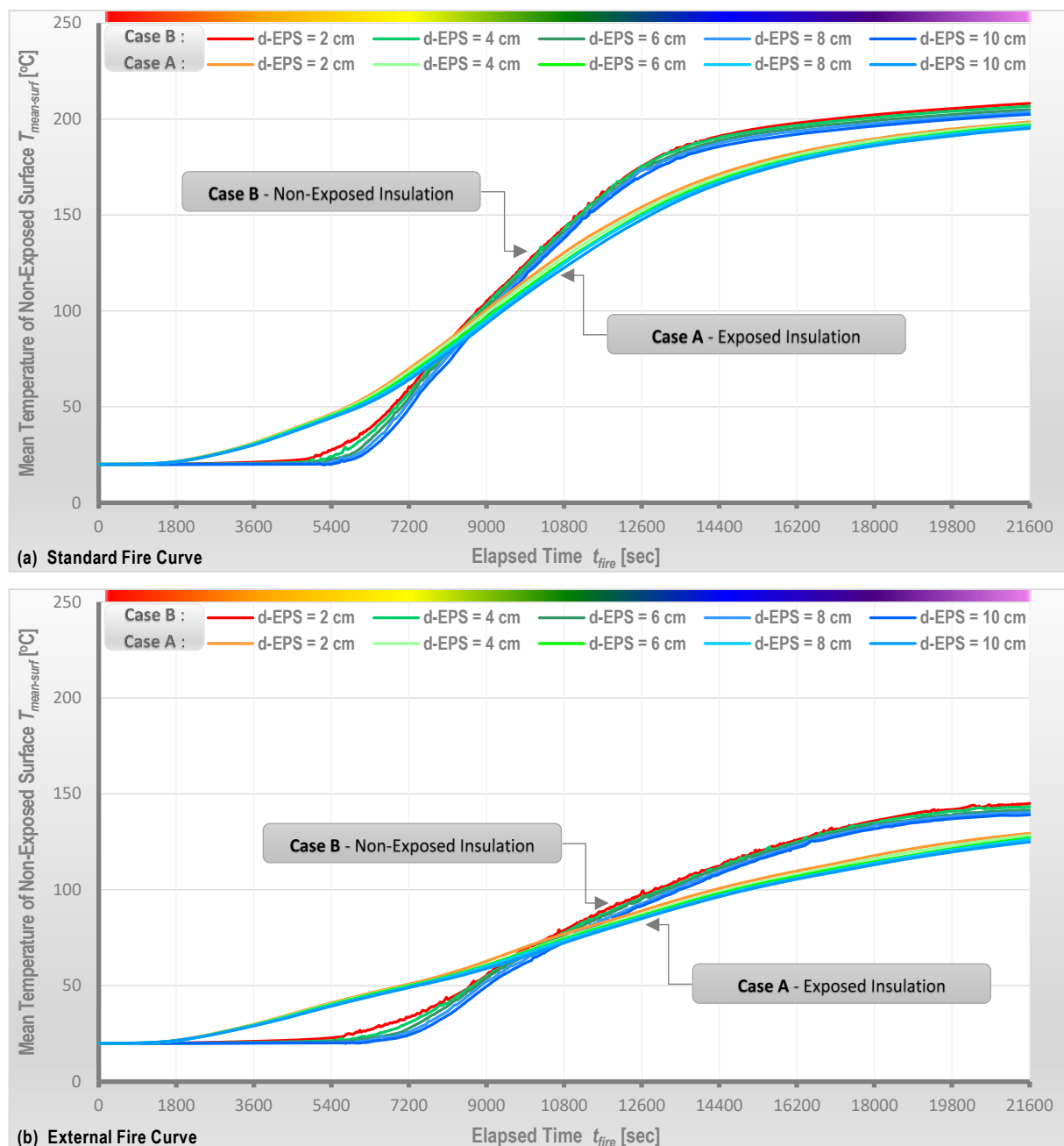


Figure 16. Temperature evolution of $T_{mean-surf}$ on the unexposed surface of the panel system, in relation with the d_{EPS} , for both studied insulation cases: (a) Standard fire curve and (b) External fire curve.

In addition to the above outcomes, it is decisive to clarify all pivotal conditions referring to the estimation of the insulation criterion. Against this background, the results in Fig. 17 further provide insights into the fluctuation of peak-surface $T_{peak-surf}$ temperature variations on the unexposed to fire side of the investigated precast element. Aiming to annihilate all obstacles inextricably linked with a robust and reliable fire analysis and in an effort to encompass extreme forcing functions in the grip of fire dynamics and within the context of the insulation criterion (I), the key findings of this research effort cast light on two illustrative nominal temperature-time curves. Results in this figure unveil an analogous temperature growth trend as before. In this regard, temperature peaks for Case A show a quicker increase as compared to Case B, while at the ending of the simulation labour exhibited temperatures almost coincide for the entire spectra of analysed cases. In this vein, temperature discrepancies for both fire actions illustrated in Fig. 17(a) and Fig. 17(b) reach up to 3.5 °C and 25 °C, respectively; tackling this issue further, it can be noticed that temperature deviations between average and peak temperatures are more dominant for Case A. In contrast, for Case B temperature deviations are lower due to a more evident normalization of temperature profiles, mostly within the mass of the unexposed to fire concrete wythe.

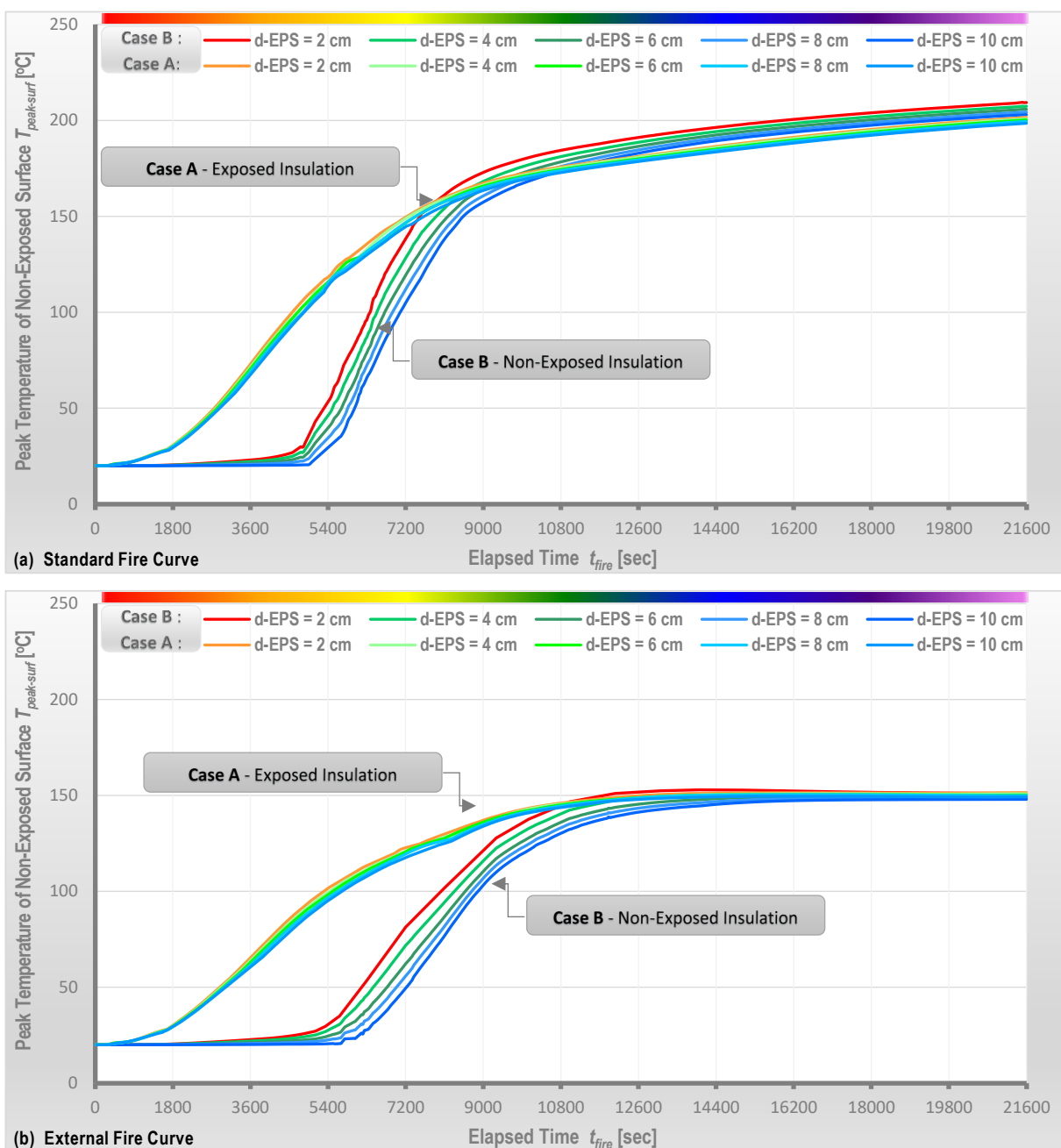


Figure 17. Temperature evolution of $T_{peak-surf}$ on the unexposed surface of the panel system, in relation with the d_{EPS} , for both studied insulation cases: (a) Standard fire curve and (b) External fire curve.

3.2. Volumetric average temperature evolution of the steel tubing coupling system between both wythes

Having addressed some cardinal issues raised over the utilisation of the thermal model to track the temperature variations of the non-exposed face of the precast concrete sandwich panel system, the rise of the volumetric average temperature of the steel tubing coupling system $T_{S235-vol}$ (between both concrete wythes) is presented on the following. Special emphasis will be put on the fire action scenario, as well as on the placement and thickness of insulation. Instantaneous temperature predictions, in relation to the aforementioned aspects, are depicted in Fig. 18(a)-(b). Before proceeding further, it is essential to bring to mind the major concerns of harmonized approaches, such as European Standards (EN). From the perspective of steel structures exposed to elevated temperatures, someone should be aware of the stress-strain relationship of carbon steel for temperatures below 400 °C [70]. As noted in EN1993-1-2, within this range the reduction factor for the effective yield strength corresponds to 1. From this angle, the present work aims to shed light on the fire performance of the panel system, while taking into account 400 °C to be the tipping point that if exceeded it may lead to premature collapse. Thus, the time point at which temperatures reach up to 400 °C might be used to identify the resistance criterion (R) of the examined system.

As can be seen, the plots in Fig. 18(a) demonstrate a swift increase of temperatures in the time domain for a Standard fire curve. This trend is certainly clear for a period of 1 ¾ hours, approximately. At this stage, volumetric average temperatures of steel tubing $T_{S235-vol}$ exceed 400 °C for both case clusters (Case A and Case B, as a function of d_{EPS}). In this behalf, the influence of d_{EPS} is shown to be slight as temperature differences for various layouts of a certain case reach up to 15 °C. Furthermore, temperature variations for Case A are higher compared to Case B; in view of this, maximum temperature deviations, reaching up to 70 °C, are presented at the final step of the analysis. In this instance, the maximum temperatures for both examined cases are approximately 600 °C and 550 °C.

From a different angle, Fig. 18(b) evinces the significance of a fire action referring to the External fire curve. This thermal attack gives rise to lower temperature variations by means of a comparison with the Standard fire curve. In this light, peak $T_{S235-vol}$ temperatures do not exceed 400 °C, while temperature deviations between both examined cases show a slighter difference. Overall, among all estimated cases and insulation thicknesses d_{EPS} the temperature divergence after 6 hours remains less than 35 °C. In addition, it should be mentioned that while for the Standard fire curve after 6 hours the average volumetric temperatures of the steel tubing coupling system are still increasing, for the External fire curve the outcome of the transient thermal analysis was rather different; as a result, after 2 hours the heat flux exchange and the corresponding resolution of temperatures remained almost constant for all settings of this fire event.

3.3. Volumetric average temperature evolution of the exposed to fire concrete wythe

In a subsequent process step, it is essential to assess the temperature field of the concrete wythe adjacent to fire, $T_{C25/30-vol}$. However, at the margin of this investigation someone should initially bear in mind European Standards (EN) and more specifically EN1992-1-2 that copes with concrete structures [69]. In this light, a loss of the resistance criterion (R) due to failure of concrete is expected for temperatures in excess of 500 °C. Based on this concept, it is necessary to evaluate the isotherms of 500 °C that underline the average depth of damaged concrete. In essence, this design procedure relies on a gradually reduced cross-section approach of concrete members subjected to a thermal action. For the aims of this investigation our major goal is to determine the volumetric average temperatures of the exposed to fire concrete wythe at each time step. This evolution somehow delineates an alternative methodology to predict the so-called loadbearing capacity of the precast system. In connection therewith, similar concerns as those raised before (types of nominal fire action, case of insulation placement and insulation thickness d_{EPS}) are illustrated in Fig. 19(a)-(b).

As noted in Fig. 19(a), the gradient of temperature rise of the analysed panel system in the vicinity of the fire source (Standard fire curve) is shown to be extremely rapid. This trend is shown to be sharp during the first two hours of fire simulations, while after this point the rate of increase is shown to be moderate. Within less than 40 min, the volumetric average temperature of the concrete wythe, corresponding to a precast element having a thermal insulation layer directly exposed to fire, reaches up to 500 °C (Case A: $R_{Case-A} \approx 40$ min). In seeking for an explanation of this trend we should firstly trust, at least with a fair confidence, the consequence of an extremely

thin concrete layer of 5 cm. Secondly, someone should bear in mind that for this case the melting of the insulation layer (EPS) leads to a fall of the rendering system (CbM) after 4 min, approximately. On the other hand, when the thermal insulation layer is positioned on the opposite side it takes less than 55 min to exceed the failure limit of the resistance criterion (Case B: $R_{Case-B} \approx 55$ min). There can be no doubt that the shown difference of $\Delta R = R_{Case-A} - R_{Case-B} = 15$ min is owing to the incombustible rendering layer, as it remains at its primary position and hinders the heat wave propagation through the volume of involved layers. Besides, it should be noted that an increase on the thickness of the combustible thermal insulation layer d_{EPS} does not change in practice the overall heat transfer process. At last, it is mentioned that the peaks of $T_{C25/30-vol}$, are close to 870 °C and 820 °C for Case A and Case B, respectively.

Along similar lines, in Fig. 19(b) we seek further to better apprehend the fire performance of the studied panel system under a less grave evolving fire (External fire curve). The central objective is to raise our awareness on the loadbearing capacity of the examined module, as a function of the severity of the fire event. As may be seen, the maximum displayed temperatures are almost 200 °C lower in contrast with the previously examined Standard fire action; accordingly, $T_{C25/30-vol}$ peaks are roughly 570 °C and 530 °C for Case A and Case B, respectively.

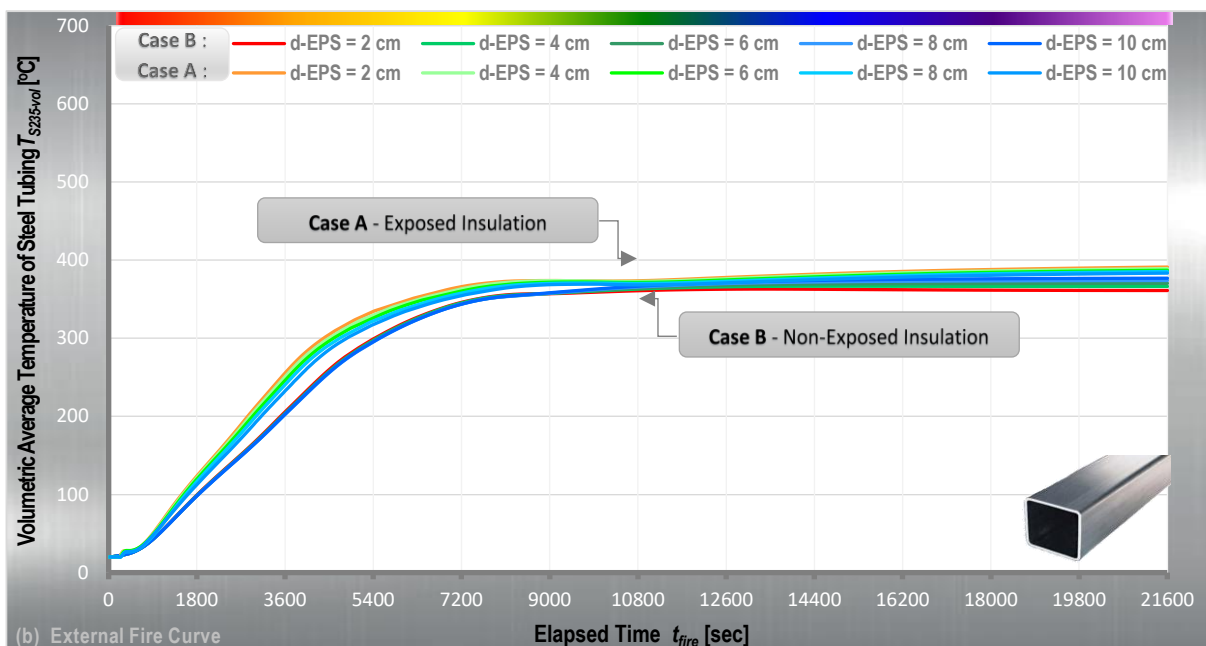
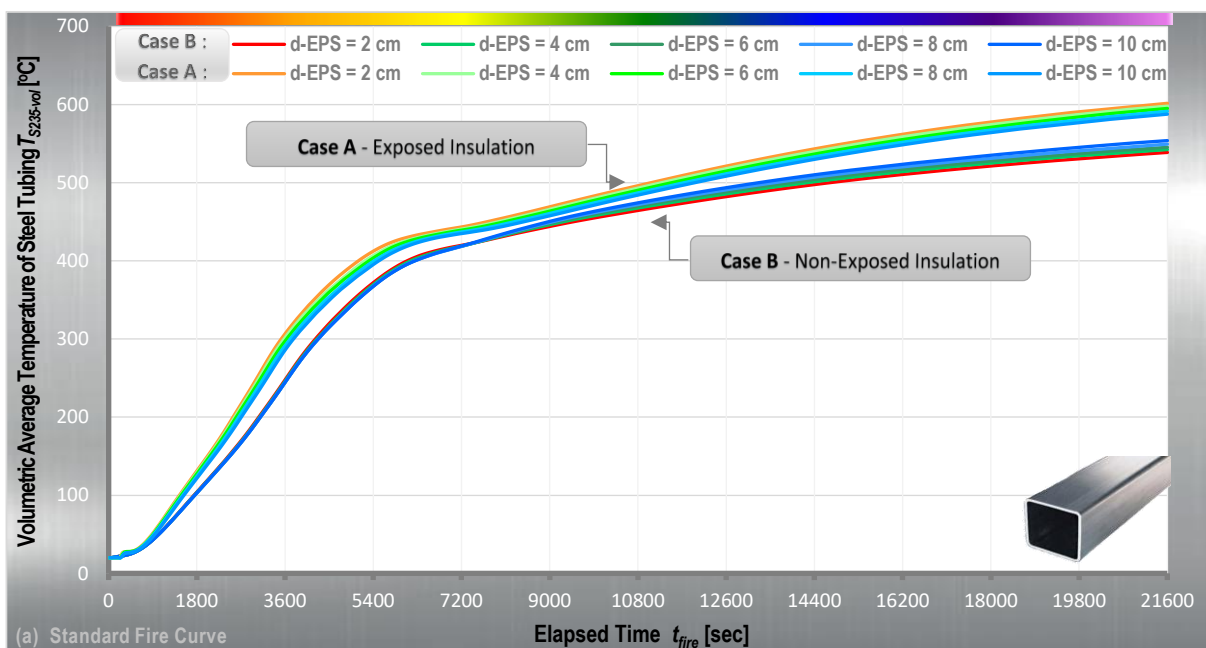


Figure 18. Volumetric average temperature variations of steel tubing $T_{S235-vol}$ between both concrete wythes, in relation with the d_{EPS} , for both studied insulation cases: (a) Standard fire curve and (b) External fire curve.

Moreover, a careful examination of the findings in this graph has revealed a diverse transient behaviour of the analysed element subjected to an External fire curve, as compared to a Standard fire curve. In that respect, plotted points in the given curves have yielded intriguing results. Thereby, the initial increasing trend of $T_{C25/30-vol}$ during the first 2 ½ hours of fire simulations, has been followed by a mild decrease of temperatures. The temperature fall mostly leans on the decomposition of insulation between both concrete plates. In this connection, the core insulation layer (combustible EPS) delineates a vigorous heat barrier that restrains the flow of heat. When this vital buffer zone is violated, absorbed heat is released (discharge of thermal capacity) and extreme temperatures striking this concrete plate are alleviated. In the long run, at the end of transient thermal simulations (after 6 hours) temperature peaks are approximately 540 °C and 500 °C for Case A and Case B, respectively. However, whilst a less severe fire threat can fundamentally support this condition, an analogous trend is not demonstrated for the ISO834 temperature-time curve as the capacity of this force is dominant.

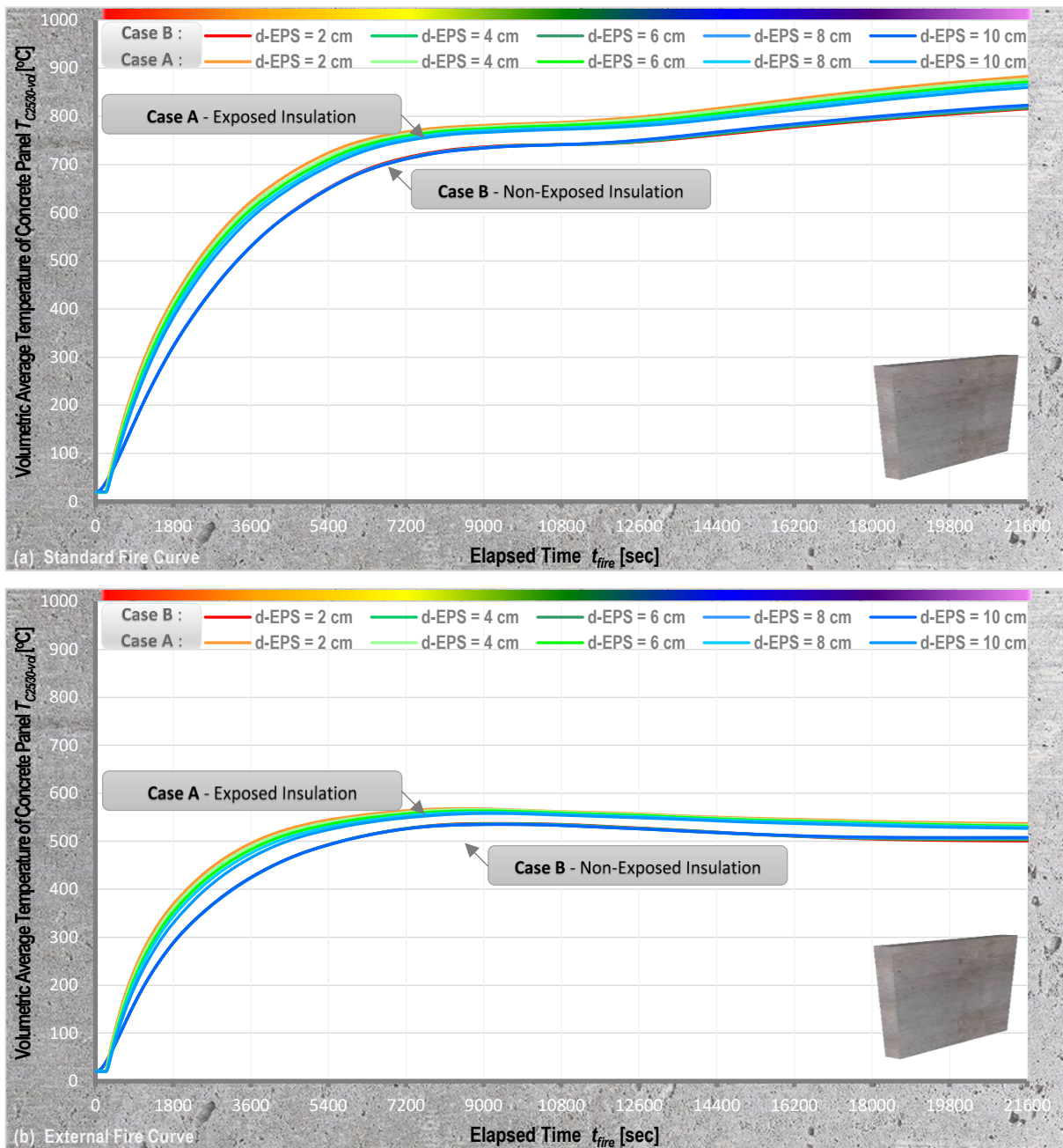


Figure 19. Volumetric average temperature variations of concrete wythe $T_{C25/30-vol}$ exposed to fire, in relation with the d_{EPS} , for both studied insulation cases: (a) Standard fire curve and (b) External fire curve.

3.4. Fire resistance predictions of analysed sandwich panel system

The adoption of the FEA and the development of a comprehensive model, as well as a highly-sophisticated elucidation of material properties in the implementation of the simulation programme have led to the aforementioned results. Based on these facts, we can identify the fire behaviour of the analysed sandwich panel system. Then again, to conceive the fire resistance of this system we could also take into account temperature evolution trends, reflecting a wide variety of possible solutions under the force of two contrasting fire hazards. In general terms, these computations aiming to reveal the fire defensiveness and responsiveness of the developed system are indicatively summarised in **Table 3**.

As can be observed, derived results underline a **satisfying level** of fire resistance, with respect to the temperature rise criterion (I) of the analysed element. In view of this, for all examined cases, this index maintains a value of more than 3 hours. On the other hand, **to tackle with the loadbearing** capacity (R) of this element, the magnitudes of this work unveil a **different situation**. For all studied cases, time intervals at which a tolerable structural response is maintained are evidently lower. Yet, fire resistance variations evince the significance of the insulation positioning. In this context, an exposed/unexposed installation of EPS to fire, alludes to higher/lower I variations and lower/higher R variations. In addition, to the urgency of this peril the reduction of temperature peaks is more obvious for the External fire curve, as compared with the Standard fire curve.

To summarise, a global decryption and visualisation of the numerical conclusion of this thermal model is given in **Fig. 20**. In that light, indicative 3D volume graphs depict the evolution of temperatures for both cases (Case A and Case B) and for both fire curves (Standard and External), while the numerical findings concern module assemblies with $d_{EPS} = 6$ cm.

Table 3. Indicative fire resistance variations of precast concrete sandwich panel system, with respect to fire curves and configuration settings.

Case Scenario	■ Standard Fire Curve			■ External Fire Curve		
	Insulation Criterion (I _{mean-surf} /I _{peak-surf}) [min]	Resistance Criterion (R _{S235-vol}) [min]	Resistance Criterion (R _{C25/30-vol}) [min]	Insulation Criterion (I _{mean-surf} /I _{peak-surf}) [min]	Resistance Criterion (R _{S235-vol}) [min]	Resistance Criterion (R _{C25/30-vol}) [min]
Cases A.1. and A.6 ● Insulation Exposed to Fire ----- $d_{EPS} = 2$ cm	219 / 203	94	40	360* / 360*	360*	62
Cases A.3. and A.8 ● Insulation Exposed to Fire ----- $d_{EPS} = 6$ cm	225 / 211	98	42	360* / 360*	360*	67
Cases A.5. and A.10 ● Insulation Exposed to Fire ----- $d_{EPS} = 10$ cm	229 / 218	103	45	360* / 360*	360*	74
Cases B.1. and B.6 ● Insulation Exposed to Air ----- $d_{EPS} = 2$ cm	194 / 166	120	55	360* / 360*	360*	95
Cases B.3. and B.8 ● Insulation Exposed to Air ----- $d_{EPS} = 6$ cm	197 / 186	121	55	360* / 360*	360*	95
Cases B.5. and B.10 ● Insulation Exposed to Air ----- $d_{EPS} = 10$ cm	199 / 199	121	55	360* / 360*	360*	95
Cases C.1. and C.2 ○ No Insulation / No Rendering ----- $d_{EPS} = 0$ cm	203 / 186	78	34	360* / 360*	360*	54

■ 0 min - 50 min,
 ■ 50 min - 100 min,
 ■ 100 min - 150 min,
 ■ 150 min - 200 min,
 ■ 200 min - 250 min,
 ■ > 300 min

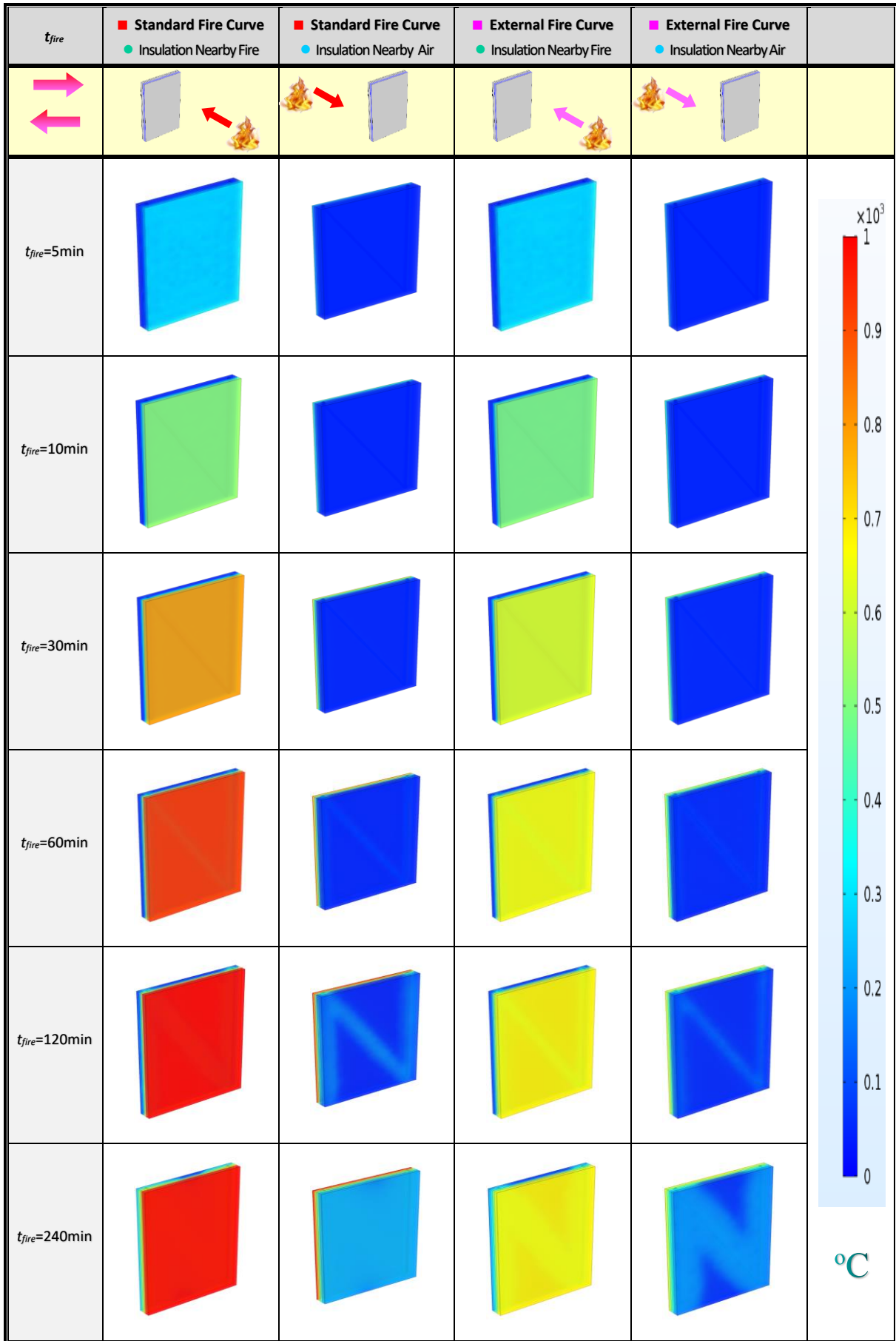


Figure 20. Volume plots of temperature progress for all considered cases and fire curve scenarios ($d_{EPS} = 6$ cm).

4. Conclusions

This work has provided new insights on the fire performance of innovative precast concrete sandwich panel systems. A FEM thermal model has been developed incorporating the modelling of temperature-dependent thermophysical properties and occurring phase changes of both combustible and non-combustible concrete sandwich panel system components to identify and interpret the effect of fire exposure on their thermal performance. The versatile numerical model has been validated against available experimental data obtained from tests performed in a large-scale vertical furnace with good qualitative and quantitative agreement. A parametric study has been performed and a variety of different datasets has been analysed, a total of twenty-two different configurations of wall arrangements, to identify the effect of positioning and width of insulation on the fire performance of the systems.

Overall, the contribution of the innovative numerical methodology can be summarised in the following points:

- A wealth of information can be provided regarding the spatial and temporal thermal distribution of precast concrete sandwich panel typologies exposed to various intensity thermal attacks under both standard and external fire curves. This approach is helping to expand our knowledge and provide detailed data regarding the concrete sandwich panel systems behaviour under fire exposure.
- Regarding the positioning of the insulation layers, the investigated panel systems with an unexposed one-side EPS insulation component revealed that the thermal transmittance rate is lower compared to the relevant panel systems having a one-side insulation directly exposed to fire conditions. It is the first time that the positioning of the insulation component is numerically investigated in [concrete sandwich panel systems](#).
- The beneficial effect of the existence of a buffer zone has also been exhibited especially after insulation layers start to melt in all systems investigated under both intense and less severe fire exposures. For all examined cases, the insulation ability (I) has been maintained for more than **3 hours** regardless of the positioning of the insulation. Further evidence though suggested that is not the case for the loadbearing capacity (R), as the installation of a fire exposed insulation layer resulted in lower stability systems.
- The effect of the insulation thickness, [ranging from 2 cm to 10 cm](#), is not that dominant as it was revealed that on average and maximum temperature deviations among marginal assemblies ($d_{EPS} = 2 \text{ cm}$ and $d_{EPS} = 10 \text{ cm}$) did not exceed $5 \text{ }^\circ\text{C}$ and $10 \text{ }^\circ\text{C}$ at $t_{fire} \approx 100 \text{ min}$, respectively.

The present work provides a framework towards understanding the thermal performance under fire conditions of precast concrete sandwich panel systems and the presented results demonstrate that there is a great potential to apply this methodology in a practical way. However, future research is planned to extend the experimental database and assess the effectiveness of the proposed numerical model to investigate an extended variety of sandwich panel systems with different insulation components and layers. [Also focus will be given to the colling stage as it would occur during a natural fire, as it is a critical aspect that has not been currently addressed in the current study.](#)

Author contributions

K.J. Kontoleon: Conceptualization, Methodology, Software, Investigation, Data Curation, Writing - Original Draft Preparation, Visualization, Supervision, Project administration. **K. Georgiadis-Filikas:** Investigation, Reviewing & Editing, Visualization. **K.G. Tsikaloudaki:** Resources, Reviewing & Editing, Funding acquisition. **T.G. Theodosiou:** Reviewing & Editing. **C.S. Giarma:** Reviewing & Editing. **C.G. Papanicolaou:** Investigation, Reviewing & Editing. **T.C. Triantafillou:** Investigation. **E.K. Asimakopoulou:** Validation, Reviewing & Editing.

All authors have read and agreed to the published version of the manuscript.

Acknowledgements

Part of this research has been co-financed by the European Regional Development Fund of the European Union and Greek national funds through the Operational Program Competitiveness, Entrepreneurship and Innovation, under the call RESEARCH – CREATE – INNOVATE (project code:T1EDK-03042). The preconstructed composite panel is part of the Greek Patent Application No. 20210100921, filed on 30-12-2021. The authors gratefully

acknowledge the technical support provided by Ph.D. candidate Mr. Kyriakos Karlos during the experimental campaign.

References

- [1] Gonçalo Correia Lopes, Romeu Vicente, Miguel Azenha, Tiago Miguel Ferreira. A systematic review of Prefabricated Enclosure Wall Panel Systems: Focus on technology driven for performance requirements. *Sustainable Cities and Society* (2018), Vol. 400, pp. 688-703. <https://doi.org/10.1016/j.scs.2017.12.027>
- [2] Jin-Ouk Choi, Xing Bin Chen, Tae Wan Kim. Opportunities and challenges of modular methods in dense urban environment. *International Journal of Construction Management* (2019), Vol. 19(2), pp. 93-105. <https://doi.org/10.1080/15623599.2017.1382093>
- [3] Khalid Najji, Murat Gunduz, Fatema Salat. Froese. Assessment of preconstruction factors in sustainable project management performance. *Engineering, Construction and Architectural Management* (2020); ISSN: 0969-9988, Emerald Publishing Limited. <https://doi.org/10.1108/ECAM-05-2020-0333>
- [4] Ravijanya Chippagiri, Hindavi R. Gavali, Rahul V. Ralegaonkar, Mike Riley, Andy Shaw, Ana Bras. Application of Sustainable Prefabricated Wall Technology for Energy Efficient Social Housing. *Sustainability* (2021), Vol. 13(3), Article Number: 1195. <https://doi.org/10.3390/su13031195>
- [5] Satheeskumar Navaratnam, Tuan Ngo, Tharaka Gunawardena, David Henderson. Performance Review of Prefabricated Building Systems and Future Research in Australia. *Buildings* (2018), Vol. 38(2), Article Number: 0038. <https://doi.org/10.3390/buildings9020038>
- [2] Richard O' Hegarty, Oliver Kinnane. Review of precast concrete sandwich panels and their innovations. *Construction and Building Materials* (2020), Vol. 233, Article Number: 117145. <https://doi.org/10.1016/j.conbuildmat.2019.117145>
- [3] Sani Mohammed Bida, Farah Nora Aznieta Abdul Aziz, Mohd Saleh Jaafar, Farzad Hejazi, Abu Bakar Nabilah. Advances in Precast Concrete Sandwich Panels toward Energy Efficient Structural Buildings. *Preprints* (2018). doi: 10.20944/preprints201810.0147.v1
- [8] M. Srivani, K. Ramadevi. Precast Wall Panel – A Review. *International Journal of Advanced Research in Science, Communication and Technology* (2020). Vol. 11(2), pp.155-159. doi: 10.48175/568
- [9] Antonella Colombo, Paolo Negro, Giandomenico Toniolo, Marco Lamperti. Design guidelines for precast structures with cladding panels. Joint Research Centre – Technical Report (2016). <https://doi.org/10.2788/956612>
- [4] Karthik Subramanya, , Sharareh Kermanshachi, Behzad Rouhanizadeh. Construction vs. Traditional Construction: Advantages and Limitations: A Comparative Study”, *Proceedings of the Creative Construction e-Conference* (2020); ISBN: 978-6-15527-061-1, pp. 10-19. <https://doi.org/10.3311/CCC2020-012>
- [5] M. Mapston, C. Westbrook. Materials for Energy Efficiency and Thermal Comfort in Buildings - Prefabricated building units and modern methods of construction (MMC) (2010); ISBN: 978-1-84569-526-2, Elsevier Ltd.: Woodhead Publishing, pp. 427-454. <https://doi.org/10.1533/9781845699277.2.427>
- [6] O. Pons. Eco-efficient Construction and Building Materials - Assessing the sustainability of prefabricated buildings (2014); ISBN: 978-0-85709-767-5, Elsevier Ltd.: Woodhead Publishing, pp. 434-456. <https://doi.org/10.1533/9780857097729.3.434>
- [7] Diana Lopez, Thomas M. Froese. Analysis of Costs and Benefits of Panelized and Modular Prefabricated Homes. *Procedia Engineering* (2016), Vol. 145, pp. 1291-1297. <https://doi.org/10.1016/j.proeng.2016.04.166>
- [8] Jeffrey Molavi, Drew L. Barral. A Construction Procurement Method to Achieve Sustainability in Modular Construction. *Procedia Engineering* (2016), Vol. 145, pp. 1362-1369. <https://doi.org/10.1016/j.proeng.2016.04.201>
- [9] Linlin Xie, Yajiao Chen, Bo Xia, Chunxiang Hua. Importance-Performance Analysis of Prefabricated Building Sustainability: A Case Study of Guangzhou. *Advances in Civil Engineering* (2020), Vol. 2020, Article Number: 8839118. <https://doi.org/10.1155/2020/8839118>
- [10] Kaicheng Shen,, Chen Cheng, Xiaodong Li, Zihui Zhang. Environmental Cost-Benefit Analysis of Prefabricated Public Housing in Beijing. *Sustainability* (2019), Vol. 11(1), Article Number: 0207. <https://doi.org/10.3390/su11010207>
- [11] I.M. Chethana S. Illankoon, Weisheng Lu. Cost implications of obtaining construction waste management-related credits in green building. *Waste Management* (2020), Vol. 102, pp. 722-731. <https://doi.org/10.1016/j.wasman.2019.11.024>
- [12] National Research Council. *Uses of Risk Analysis to Achieve Balanced Safety in Building Design and Operations* (1991); ISBN: 978-0-309-04680-0, The National Academies Press; Washington, DC - USA. <https://doi.org/10.17226/1907>
- [13] Rita Yi Man Li, Kwong Wing Chau, Frankie Fanjie Zeng. Ranking of Risks for Existing and New Building Works. *Sustainability* (2019), Vol. 11(10), Article Number: 2863. <https://doi.org/10.3390/su11102863>
- [14] Pēteris Druķis, Līga Gaile, Leonīds Pakrašiņš. Inspection of Public Buildings Based on Risk Assessment. *Procedia Engineering* (2017), Vol. 172, pp. 247-255. <https://doi.org/10.1016/j.proeng.2016.04.166>
- [15] Kate T.Q. Nguyen, Satheeskumar Navaratnam, Priyan Mendis, Kevin Zhang, Jonathan Barnett, Hao Wang. Fire safety of composited in prefabricated buildings: From fibre reinforced polyper to textile concrete. *Composites Part B: Engineering* (2020) Vol. 187, Article Number: 107815. <https://doi.org/10.1016/j.compositesb.2020.107815>
- [16] Venkatesh Kodur, Puneet Kumar. Fire hazard in buildings: review, assessment and strategies for improving fire safety. *Emerald Insight* (2020), Vol.4(1), pp. 1-23. doi: 10.1108/PRR-12-2018-0033
- [17] C. M. Benson, S. Elsmor. Reducing fire risk in buildings: the role of fire safety expertise and governance in building and planning approval. *Journal of Housing and the Built Environment* (2021). <https://doi.org/10.1007/s10901-021-09870-9>

- [18] Guo-Qiang Li, Chao Zhang. A Review on Fire Safety Engineering: Key Issues for High-Rise Buildings. *International Journal of High-Rise Buildings* (2017), Vol. 7(4), pp. 265-285. <https://doi.org/10.21022/IJHRB.2018.7.4.265>
- [19] Yaping He. Probabilistic fire-risk-assessment function and its application in fire resistance design. *Procedia Engineering* (2013), Vol. 62, pp. 130-139. <https://doi.org/10.1016/j.proeng.2013.08.050>
- [20] Yaping He, Stephen Grubits. A Risk-based Equivalence Approach to Fire Resistance Design for Buildings. *Journal of Fire Protection Engineering* (2010), Vol. 20(1), pp.5-26. <https://doi.org/10.1177/1042391509360306>
- [21] Spencer Chainey. Using the vulnerable localities index to identify priority areas for targeting fire safety services. *Fire Safety Journal* (2013), Vol. 62(Part A), pp. 30-36. <https://doi.org/10.1016/j.firesaf.2013.03.013>
- [22] Jing Xin, Chong Fu Huang. Fire risk analysis of residential buildings based on scenario clusters and its application in fire risk management. *Fire Safety Journal* (2013), Vol. 62(Part A), pp. 72-78. <https://doi.org/10.1016/j.firesaf.2013.09.022>
- ~~[29] Jing Xin, Chong Fu Huang. Fire Risk Assessment of Residential Buildings Based on Fire Statistics from China. *Fire Technology* (2014), Vol. 50, pp. 1147-1161. <https://doi.org/10.1007/s10694-013-0227-8>~~
- [23] Gabriele Bernardini. SpringerBriefs in Applied Sciences and Technology, In: Janusz Kacprzyk, Editor. *Fire Safety of Historical Buildings - Traditional Versus Innovative "Behavioural Design" Solutions by Using Wayfinding Systems* (2017); ISBN: 978-3-319-55743-4, Springer Nature; Switzerland AG. <https://doi.org/10.1007/978-3-319-55744-1>
- [24] John M. Watts Jr., Marilyn E. Kaplan. Fire Risk Index for Historic Buildings. *Fire Technology* (2001), Vol. 37, pp. 167-180. <https://doi.org/10.1023/A:1011649802894>
- [25] J.L. Torero. Fire Safety of Historical Buildings: Principles and Methodological Approach. *Journal of Architectural Heritage* (2019), Vol. 13(7), pp. 926-940. <https://doi.org/10.1080/15583058.2019.1612484>
- [26] Jane Lotaile. *Fire Protection Engineering in Building Design* (2003); ISBN: 978-0-7506-7497-3, Elsevier Ltd.: Butterworth-Heinemann. <https://doi.org/10.1016/B978-0-7506-7497-3.X5000-0>
- [27] Margrethe Kobes, Ira Helsloot, Bauke de Vries, Jos G.Post. Building safety and human behaviour in fire: A literature review. *Fire Safety Journal* (2010), Vol. 45(1), pp. 1-11. <https://doi.org/10.1016/j.firesaf.2009.08.005>
- [28] Débora M.Ferreira, Alexandre Araújo, Elza M.M.Fonseca, Paulo A.G.Piloto, Jorge Pintoc. Behaviour of non-loadbearing tabique wall subjected to fire – Experimental and numerical analysis. *Journal of Building Engineering* (2017), Vol. 9, pp. 164-176. <https://doi.org/10.1016/j.job.2016.11.003>
- ~~[36] Maina Kironji. Evaluation of Fire Protection Systems in Commercial Highrise Buildings for Fire Safety Optimization – A Case of Nairobi Central Business District. *International Journal of Scientific and Research Publications* (2015), Vol. 5(10), pp. 1-11. doi:10.13140/RG.2.2.21562.64965~~
- [29] Adam Cowlard, Adam Bittern, Cecilia Abecassis-Empis, José Torero. Fire Safety Design for Tall Buildings. *Procedia Engineering* (2013), Vol. 62, pp. 169-181. <https://doi.org/10.1016/j.proeng.2013.08.053>
- [30] Morgan J. Hurley, Eric R. Rosenbaum. *Performance-Based Fire Safety Design* (2015); ISBN: 978-0-367-87027-0, CRC Press - Taylor & Francis Group; Boca Raton - USA. <https://doi.org/10.1201/b18375>
- [31] A. Alvarez, B.J. Meacham, N.A. Dembsy, J.R. Thomas. Twenty years of performance-based fire protection design: challenges faced and a look ahead. *Journal of Fire Protection Engineering* (2013), Vol.23(4), pp. 249-276. <https://doi.org/10.1177/1042391513484911>
- ~~[40] Said M. Easa, Wai Yeung Yan. Performance-Based Analysis in Civil Engineering: Overview of Applications. *Infrastructures* (2019), Vol. 4(2), Article Number: 0028. <https://doi.org/10.3390/infrastructures4020028>~~
- [32] Greg Baker, Colleen Wade, Michael Spearpoint, Charley Fleischmann. Developing Probabilistic Design Fires for Performance-based Fire Safety Engineering. *Procedia Engineering* (2013), Vol. 62, pp. 639-647. <https://doi.org/10.1016/j.proeng.2013.08.109>
- ~~[42] Wanki Chow. Experience on Implementing Performance-based Design in Hong Kong. *Procedia Engineering* (2013), Vol. 62, pp. 28-35. <https://doi.org/10.1016/j.proeng.2013.08.041>~~
- [33] Thomas Gernay, Negar Elhami Khorasani. Recommendations for performance-based fire design of composite steel buildings using computational analysis. *Journal of Constructional Steel Research* (2020), Vol. 166, Article Number: 105906. <https://doi.org/10.1016/j.jcsr.2019.105906>
- [34] Won-Keel Hong. *Hybrid Composite Precast Systems* (2020); ISBN: 978-0-081-02721-9, Elsevier Ltd.: Woodhead Publishing. <https://doi.org/10.1016/C2017-0-04395-1>
- [35] Qing Zhi, Zhengxing Guo. Experimental evaluation of precast concrete sandwich wall panels with steel-glass fiber-reinforced polymer shear connectors. *Advances in Structural Engineering* (2017), Vol. 20(10), pp. 1476-1492. <https://doi.org/10.1177/1369433216683198>
- [36] Oliver Kinnane, Roger West, Richard O' Hegarty. Structural shear performance of insulated precast concrete sandwich panels with steel plate connectors. *Engineering Structures* (2020), Vol. 215, Article Number: 110691. <https://doi.org/10.1016/j.engstruct.2020.110691>
- [37] Richard O' Hegarty, Oliver Kinnane, Michael Grimes, John Newell, Michael Clifford, Roger West. Development of thin precast concrete sandwich panels: Challenges and outcomes. *Construction and Building Materials* (2021), Vol. 267, Article Number: 120981. <https://doi.org/10.1016/j.conbuildmat.2020.120981>
- [38] T. Voellinger, A. Bassi, M. Heitel. Facilitating the incorporation of VIP into precast concrete sandwich panels. *Energy and Buildings* (2014), Vol. 85, pp. 666-671. <https://doi.org/10.1016/j.enbuild.2014.05.038>

- [39] Jun Chen, Ehab Hamed, R. Ian Gilbert. Structural performance of concrete sandwich panels under fire. *Fire Safety Journal* (2021), Vol. 121, Article Number: 103293. <https://doi.org/10.1016/j.firesaf.2021.103293>
- [40] Thanyawat Pothisiri, Pitcha Jongvivatsakul, Soklin Chou, Anil C. Wijeyewickrema. Modeling of Precast Concrete Load-Bearing Walls Exposed to Fire. *Engineering Journal* (2019), Vol. 23(6), pp. 433-449. <https://doi.org/10.4186/ej.2019.23.6.433>
- [41] Linus C S Lim, Andrew H Buchanan. Fire Behaviour of Slender Precast Concrete Walls. *Fire Safety Science* (2003), Vol. 7, pp. 1135-1146. doi:10.3801/IAFSS.FSS.7-1135
- [42] Thomas Hulin, Kamil Hodicky, Jacob W. Schmidt, Henrik Stang. Experimental investigations of sandwich panels using high performance concrete thin plates exposed to fire. *Materials and Structures* (2016), Vol. 49, pp. 3879–3891. <https://doi.org/10.1617/s11527-015-0760-x>
- [43] Haoming Xu, Min Yu, Congcong Xue, Lihua Xu, Jianqiao Ye. Experimental study on fire resistance of precast concrete columns with efficient reinforcement. *Engineering Structures* (2020), Vol. 204, Article Number: 109947. <https://doi.org/10.1016/j.engstruct.2019.109947>
- [44] EN1363-1 (2020): Fire resistance tests - Part 1: General requirements, European Standard.
- [45] ISO834-1 (1999): Fire-resistance tests - Elements of building construction - Part 1: General requirements, International Standards Organisation.
- [46] Thadshajini Suntharalingam, Perampalam Gatheeshgar, Irindu Upasiri, Keerthan Poolaganathan, Brabha Nagaratnam, Marco Corradi, Dilini Nuwanthika. Fire performance of innovative 3D printed concrete composite wall panels - A Numerical Study. *Case Studies in Construction Materials* (2021), Vol. 15, Article Number: e00586. <https://doi.org/10.1016/j.cscm.2021.e00586>
- [47] Diogo Pereira, António Gago, Jorge Proença, Tiago Morgado. Fire performance of sandwich wall assemblies. *Composites Part B: Engineering* (2016), Vol. 93, pp. 123-131. <https://doi.org/10.1016/j.compositesb.2016.03.001>
- [48] Michel Murillo A., Bernardo F. Tutikian, Vinicius Ortolan, Marcos L.S. Oliveira, Carlos H. Sampaio, Leandro Gómez P., Luis F. Silva O. Fire resistance performance of concrete-PVC panels with polyvinyl chloride (PVC) stay in place (SIP) formwork. *Journal of Materials Research and Technology* (2019), Vol. 8(5), pp. 4094-4107. <https://doi.org/10.1016/j.jmrt.2019.07.018>
- ~~[59] PyroSim Simulation Software – User Manual, Version 2021.3, Thunderhead Engineering, Inc. (www.thunderheadeng.com/pyrosim).~~
- [49] Thomas Gernay and Panos Kotsovinos. Chapter 10 - Advanced Analysis, In: Kevin LaMalva, Danny Hopkin, Editors. *International Handbook of Structural Fire Engineering* (2021); ISBN: ISBN: 978-3-030-77123-2, Springer Nature Switzerland AG, pp. 413-467. https://doi.org/10.1007/978-3-030-77123-2_10
- ~~[61] Yavor Panev, Panagiotis Kotsovinos, Susan Deeny, Graeme Flint. The Use of Machine Learning for the Prediction of fire Resistance of Composite Shallow Floor Systems. *Fire Technology* (2021). <https://doi.org/10.1007/s10694-021-01108-y>~~
- [50] EN1991-1-2 (2002), Eurocode 1: Actions on Structures - Part 1-2: General Actions - Actions on Structures Exposed to Fire, European Standard.
- [51] COMSOL Multiphysics® Simulation Software - Reference Manual, Version 5.3a, COMSOL, Inc. (www.comsol.com).
- [52] Paudel, D., Rinta-Paavola, A., Mattila, HP., Hostikka, S., Multiphysics Modelling of Stone Wool Fire Resistance. *Fire Technology* 57, 1283–1312 (2021) <https://doi.org/10.1007/s10694-020-01050-5>
- [53] Witkowski, A., Girardin, B., Försth, M., Hewitt, F., Fontaine, G., Duquesne, S., Bourbigot, S., Hull, R., Development of an anaerobic pyrolysis model for fire retardant cable sheathing materials, *Polymer Degradation and Stability* 113, 208-217 (2015) <https://doi.org/10.1016/j.polymdegradstab.2015.01.006>.
- [54] Morgan J. Hurley. *SFPE Handbook of Fire Protection Engineering* (2016); ISBN: 978-1-4939-2564-3, Springer Science: SFPE. <https://doi.org/10.1007/978-1-4939-2565-0>
- [55] Angus Law, Luke Bisby. The rise and rise of fire resistance. *Fire Safety Journal* (2020), Vol. 116, Article Number: 103188. <https://doi.org/10.1016/j.firesaf.2020.103188>
- [56] Simon H. Ingberg. Test of the severity of building fires. *National Fire Protection Association Quarterly* (1928), Vol. 22, pp. 43-61.
- [57] Thanyawat Pothisiri, Chou Soklin. Effects of Mixing Sequence of Polypropylene Fibers on Spalling Resistance of Normal Strength Concrete. *Engineering Journal* (2013), Vol. 18(3), pp. 55-63. <https://doi.org/10.4186/ej.2014.18.3.55>
- [58] Nils Johansson. Numerical experiments and compartment fires. *Fire Science Reviews* (2014), Vol. 3(2). <https://doi.org/10.1186/s40038-014-0002-2>
- [59] M.Z. Naser. Mechanistically Informed Machine Learning and Artificial Intelligence in Fire Engineering and Sciences. *Fire Technology* (2021). <https://doi.org/10.1007/s10694-020-01069-8>
- [60] L. Sousa, C.F. Castro, C.C. António, H. de Sousa, R. Sousa. The design, properties and performance of shape optimized masonry blocks, In: F. Pacheco-Torgal, P.B. Lourenço, J.A. Labrincha, S. Kumar, P. Chindaprasirt, Editors. *Eco-Efficient Masonry Bricks and Blocks - Design, Properties and Durability* (2015); ISBN: 978-1-78242-305-8, Elsevier Ltd.: Woodhead Publishing, pp. 249-269. <https://doi.org/10.1016/C2014-0-02158-2>
- [61] Guan Heng Yeoh, Kwok Kit Yuen. *Computational fluid dynamics in fire engineering - Theory, modelling and practice* (2009); ISBN: 978-0-75068-589-4, Elsevier Ltd.: Butterworth-Heinemann. <https://doi.org/10.1016/B978-0-7506-8589-4.X0001-4>
- [62] Frank P. Incropera, David P. DeWitt, Theodore L. Bergman, Adrienne S. Lavine. *Fundamentals of heat and mass transfer* (1996); ISBN-13: 978-0-4714-5728-2, John Wiley & Sons, Inc.

- [63] Yunus A. Cengel. *Heat transfer - A Practical Approach* (2003); ISBN 10: 0070115052 & ISBN-13: 978-0-0701-1505-7, McGraw - Hill, Inc.
- [74] James L. Threlkeld. *Thermal Environmental Engineering* (1970); Prentice-Hall, Englewood Cliffs, Inc: New Jersey, USA.
- [75] Rufus Oldenburger. *Mathematical Engineering Analysis* (1950); Dover Publications, Inc: New York, USA.
- [76] Thomas Blomberg. *Heat conduction in two and three dimensions – Computer modelling of building physics applications* (1996); Report TVBH-1008, ISRN LUTVDG/TVBH-96/1008-SE/(1-188) ISBN 91-88722-05-8, Department of Building Physics, Lund University, Sweden.
- [64] John H. Lienhard IV, John H. Lienhard V. *A heat transfer textbook* (2000); Cambridge MA, USA.
- [65] K.G. Tsikaloudaki, T.G. Theodosiou, C.S. Giarma, K.J. Kontoleon, D.G. Aravantino, S.P. Tsoka, D.C. Tsirigoti, P.D. Chastas, A.C. Karaoulis. *Advancing sustainability in prefabricated buildings*. IOP Conference Series: Earth and Environmental Science (2020); World Sustainable Built Environment - Beyond 2020, WSBE 2020Gothenburg (Sweden), Vol. 588(5), Article Number: 052067. <https://doi.org/10.1088/1755-1315/588/5/052067>
- [66] T.G. Theodosiou, K.G. Tsikaloudaki, K.J. Kontoleon, C.S. Giarma. *Assessing the accuracy of predictive thermal bridge heat flow methodologies*. Renewable and Sustainable Energy Reviews (2021), Vol. 136, Article Number: 110437. <https://doi.org/10.1016/j.rser.2020.110437>
- [67] Hellenic National Regulation on the Energy Performance of Buildings (REPB), Ministerial Decision (2010). Hellenic Ministry of Environment, Energy and Climate Change Official Journal of the Hellenic Republic (FEK) 407-B/09-04-2010, 24 p., April 2010 [in Greek].
- [68] Technical Guideline of Technical Chamber of Greece (TOTE 20701-2/2017): *Thermophysical Properties of Building Envelope Elements and Evaluation of the Thermal Insulation Adequacy of Buildings* (2017). Technical Chamber of Greece (TEE), Hellenic Ministry of Environment Energy and Climate Change (HMECC) Official Journal of the Hellenic Republic (FEK) 4003-B/17-11-2017, 90 p., September 2017 [in Greek].
- [69] EN1992-1-2 (2004), Eurocode 2: Design of Concrete Structures - Part 1-2: General Rules - Structural Fire Design, European Standard.
- [70] EN1993-1-2 (2005), Eurocode 3: Design of Steel Structures - Part 1-2: General Rules - Structural Fire Design, European Standard.
- [71] K. Georgiadis-Filikas. *Behaviour of thermal insulation materials under fire conditions with reference to their position within building envelopes*. Ph.D. Thesis (2015), Aristotle University of Thessaloniki, Greece, ND: 35980 [in Greek]. <http://hdl.handle.net/10442/hedi/35980>
- [72] V. Babrauskas. *Sandwich Panel Performance in Full-scale and Bench-scale Fire Tests*. Fire Materials (1997), Vol. 21, pp. 53-65. [https://doi.org/10.1002/\(SICI\)1099-1018\(199703\)21:2<53::AIDFAM593>3.0.CO;2-8](https://doi.org/10.1002/(SICI)1099-1018(199703)21:2<53::AIDFAM593>3.0.CO;2-8).
- [73] P. Blomqvist, M. Simonson-McNamee, P. Thureson. *Compilation of International Building Regulations (Fire) Relevant for EPS/XPS, SP* Technical Research Institute of Sweden, Borås, 2010.
- [74] G. Griffin, A. Bicknell, G. Bradbury, N. White. *Effect of Construction Method on the Fire Behavior of Sandwich Panels with Expanded Polystyrene Cores in Room Fire Tests*. Journal of Fire Sciences (2006), Vol. 24, pp. 275-294. <https://doi.org/10.1177/0734904106059052>.
- [75] C. Bouster, P. Vermande, J. Veron. *Study of the pyrolysis of polystyrenes*. Journal of Analytical and Applied Pyrolysis (1980), Vol. 1, pp. 297-313. [https://doi.org/10.1016/0165-2370\(80\)80014-3](https://doi.org/10.1016/0165-2370(80)80014-3).
- [76] S. Mehta, S. Biederman, S. Shivkumar. *Thermal degradation of foamed polystyrene*. Journal of Material Sciences (1995), Vol. 30, pp. 2944-2949. <https://doi.org/10.1007/BF00349667>
- [77] A. Marcilla, M. Beltrán. *Kinetic study of the thermal decomposition of polystyrene and polyethylene-vinyl acetate graft copolymers by thermogravimetric analysis*. Polymer Degradation and Stability (1995), Vol. 50, pp. 117-124. [https://doi.org/10.1016/0141-3910\(95\)00138-C](https://doi.org/10.1016/0141-3910(95)00138-C).
- [78] M. Sands, S. Shivkumar. *EPS molecular weight and foam density effects in the lost foam process*. Journal of Material Sciences (2003), Vol. 38, pp. 2233-2239.
- [79] Q. Xu, C. Jin, G. Griffin, Y. Jiang. *Fire safety evaluation of expanded polystyrene foam by multi-scale methods*. Journal of Thermal Analysis and Calorimetry (2013), Vol. 115, pp. 1651-1660. <https://doi.org/10.1007/s10973-013-3431-6>.
- [80] A. Dawson, M. Rides, C. Allen. *NPL Report MAT 7. The Measurement of the Thermal Conductivity of Amorphous Polymers Above Glass Transition Temperature*. Teddington, Middlesex, 2007.
- [81] EN1364-1 (2019), *Fire resistance tests for non-loadbearing elements - Part 1: Walls*, European Standard.
- [82] K.J. Kontoleon, T.G. Theodosiou, K.G. Tsikaloudaki. *The influence of concrete density and conductivity on walls' thermal inertia parameters under a variety of masonry and insulation placements*. Applied Energy (2013), Vol. 112, pp. 325-337. <https://doi.org/10.1016/j.apenergy.2013.06.029>

Highlights of Manuscript

In overall, 5 Bullet Points (maximum 85 characters, including spaces, per bullet point)

- Thermal analysis of precast concrete sandwich wall system exposed to a fire attack.
- Adoption of temperature-dependent material properties under elevated temperatures.
- Modelling technique for numerical treatment of EPS decomposition and render fall.
- FEA-based simulations with respect to the thickness and position of EPS insulation.
- Validation of the model and degree of agreement by means of a medium-scale test.

List of Figure Captions

In overall, 20 Figures

Figure 1. Fire resistance criteria (R, E, I) of building components, from a passive design perspective.

Figure 2. Outline of heat transfer mechanisms, with respect to the examined precast concrete sandwich panel subjected to a fire threat.

Figure 3. Analysed nominal temperature-time curves indicated in Eurocode 1 (EN1991-1-2): (a) Standard fire curve; (b) External fire curve.

Figure 4. General layout and views of the developed precast concrete sandwich panel system.

Figure 5. Horizontal cross-sections of precast concrete sandwich panel system (XZ view), with a varying thickness of the one-side insulation layer (d_{EPS}).

Figure 6. Modelling of temperature-dependent thermophysical properties of non-combustible materials (C25/30, CbM and S235).

Figure 7. Modelling of temperature-dependent thermophysical properties of combustible material (EPS, for both possible placements).

Figure 8. (a) Temperature evolution at the interface upon contact of both layers (CbM and EPS); (b)-(d) Modelling of time dependent thermophysical properties of insulated render, directly exposed to a fire action.

Figure 9. Modelling of temperature-dependent thermal emissivity of basic material surfaces (C25/30, CbM and S235) of the precast system.

Figure 10. Three-dimensional modelling and meshing arrangement of the thermal probe, reflecting heat transfer processes through a precast concrete sandwich panel system, by using COMSOL Multiphysics® simulation software.

Figure 11. Experimental configuration of the embedded specimens in a walled metal steel frame in the large-scale furnace (specimen of interest: the one on the left).

Figure 12. Schematic of the positioning of the thermocouples (left) and positioning of the thermocouples on the unexposed surface of the specimen (right).

Figure 13. Measurements and model predictions of the temperature of the unexposed surface.

Figure 14. Dehydration (left, as manifested on the specimen placed on the right of the frame) and hairline cracking (right) during the test.

Figure 15. Unexposed surface temperature 93 min (left) and 188 min (right) after fire initiation.

Figure 16. Temperature evolution of $T_{mean-surf}$ on the unexposed surface of the panel system, in relation with the d_{EPS} , for both studied insulation cases: (a) Standard fire curve and (b) External fire curve.

Figure 17. Temperature evolution of $T_{peak-surf}$ on the unexposed surface of the panel system, in relation with the d_{EPS} , for both studied insulation cases: (a) Standard fire curve and (b) External fire curve.

Figure 18. Volumetric average temperature variations of steel tubing $T_{S235-vol}$ between both concrete wythes, in relation with the d_{EPS} , for both studied insulation cases: (a) Standard fire curve and (b) External fire curve.

Figure 19. Volumetric average temperature variations of concrete wythe $T_{C25/30-vol}$ exposed to fire, in relation with the d_{EPS} , for both studied insulation cases: (a) Standard fire curve and (b) External fire curve.

Figure 20. Volume plots of temperature progress for all considered cases and fire curve scenarios ($d_{EPS} = 6$ cm).

List of Table Captions

In overall, 3 Tables

Table 1. Thermophysical properties of concerned materials subjected to a conventional and steady-state of temperature variations (20 °C).

Table 2. Datasets of analysed precast system, with respect to investigated parameters.

Table 3. Indicative fire resistance variations of precast concrete sandwich panel system, with respect to fire curves and configuration settings.